
Policy-Driven World Model Adaptation for Robust Offline Model-based Reinforcement Learning

Jiayu Chen

Carnegie Mellon University
School of Computer Science
jiayuc2@andrew.cmu.edu

Aravind Venugopal

Carnegie Mellon University
School of Computer Science
avenugo2@andrew.cmu.edu

Jeff Schneider

Carnegie Mellon University
School of Computer Science
jeff4@andrew.cmu.edu

Abstract

Offline reinforcement learning (RL) offers a powerful paradigm for data-driven control. Compared to model-free approaches, offline model-based RL (MBRL) explicitly learns a world model from a static dataset and uses it as a surrogate simulator, improving data efficiency and enabling potential generalization beyond the dataset support. However, most existing offline MBRL methods follow a two-stage training procedure: first learning a world model by maximizing the likelihood of the observed transitions, then optimizing a policy to maximize its expected return under the learned model. This objective mismatch results in a world model that is not necessarily optimized for effective policy learning. Moreover, we observe that policies learned via offline MBRL often lack robustness during deployment, and small adversarial noise in the environment can lead to significant performance degradation. To address these, we propose a framework that dynamically adapts the world model alongside the policy under a unified learning objective aimed at improving robustness. At the core of our method is a maximin optimization problem, which we solve by innovatively utilizing Stackelberg learning dynamics. We provide theoretical analysis to support our design and introduce computationally efficient implementations. We benchmark our algorithm on twelve noisy D4RL MuJoCo tasks and three stochastic Tokamak Control tasks, demonstrating its state-of-the-art performance.

1 Introduction and Related Works

Offline RL [1] leverages offline datasets of transitions, collected by a behavior policy, to train a policy. To avoid overestimation of the expected return for out-of-distribution states, which can mislead policy learning, model-free offline RL methods [2, 3] often constrain the learned policy to remain close to the behavior policy. However, acquiring a large volume of demonstrations from a high-quality behavior policy, can be expensive. This challenge has led to the development of offline model-based reinforcement learning (MBRL) approaches, such as [4, 5, 6]. These methods train dynamics models from offline data and optimize policies using imaginary rollouts simulated by the models. Notably, the dynamics modeling is independent of the behavior policy, making it possible to learn effective policies from any behavior policy that reasonably covers the state-action spaces.

As detailed in Section 2, offline MBRL typically follows a two-stage framework: first, learning a world model by maximizing the likelihood of transitions in the offline dataset; and second, using the learned model as a surrogate simulator to train RL policies. Unlike in online MBRL [7, 8, 9], the world model in offline settings is typically not adapted alongside the policy. Moreover, the model training objective, i.e., likelihood maximization, differs from the goal of policy optimization, i.e., maximizing the expected return, leading to the issue of objective mismatch [10]. There has been extensive research addressing this mismatch in online MBRL (e.g., [11, 12, 13, 14, 15, 16]), primarily

by directly optimizing the model to increase the current policy’s return in the environment. However, applying these strategies in the offline setting can be problematic. Since the real environment is inaccessible during offline training, optimizing the world model solely to increase returns in imagined rollouts can cause it to diverge from the true dynamics, thereby misleading the policy updates. Comparisons between [17] and [5] show that, for offline MBRL, return-driven model adaptation can underperform approaches that do not dynamically update the world model. **How to adapt the world model alongside the policy under a unified objective remains an open challenge in offline MBRL.** In this paper, we propose such a unified training framework to learn robust RL policies from offline data. Specifically, the objective is formulated as a maximin problem: we maximize the worst-case performance of the policy, where the policy seeks to maximize its expected return while the world model is updated adversarially to minimize it. This direction of model updating is opposite to that used in online MBRL, as conservatism is critical in offline RL [1].

Another motivation behind our algorithm design is that the state-of-the-art model-free and model-based offline RL algorithms lack robustness during deployment, as demonstrated in Figure 1, as the learned policies often overfit to the static dataset or data-driven dynamics models. Changing the objective to maximizing the worst-case performance of the policy can potentially mitigate such issues. While several theoretical studies have investigated robustness in (model-based) RL [18, 19, 20, 21], the proposed algorithms are not scalable to high-dimensional continuous control tasks. The work most closely related to ours is RAMBO [22], which also targets robust offline MBRL. However, RAMBO does not formulate the problem as a Stackelberg game, where the policy and world model act as leader and follower in a general-sum game. Also, it does not employ Stackelberg learning dynamics [23, 24, 25, 26], which are essential for solving the maximin optimization inherent in robust RL (see Section 2 for details). Additionally, since the world model is updated jointly with the policy, historical rollouts in the replay buffer would become outdated for policy training due to distributional shift. While RAMBO overlooks this issue, we introduce a novel gradient mask mechanism (detailed in Appendix J) to mitigate it while preserving training efficiency.

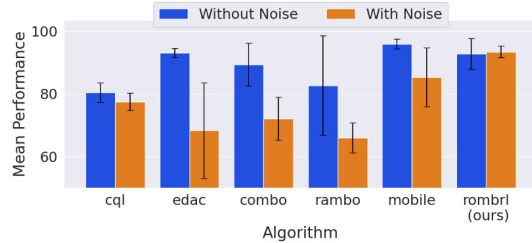


Figure 1: Average scores of different offline RL algorithms on nine D4RL MuJoCo tasks (corresponding to the tasks in Table 1 excluding those with the random data type), before and after applying random noise to state transitions. The noise is modeled as zero-mean Gaussian with a standard deviation equal to 5% of the state change, simulating common measurement noise.

Our contributions are as follows: (1) We propose a novel offline MBRL algorithm (ROMBRL) that jointly optimizes the model and policy for robustness by solving a constrained maximin optimization problem. We further provide novel theoretical guarantees on the suboptimality gap of the resulting robust policy. (2) To solve this maximin problem, we model it as a Stackelberg game and introduce novel Stackelberg learning dynamics for stochastic gradient updates of the policy and model. To the best of our knowledge, this is the first application of the Stackelberg game framework to offline MBRL. (3) We develop practical implementations of the proposed learning dynamics, including the use of the Woodbury matrix identity for efficient second-order gradient computation and a gradient-mask mechanism that enables off-policy training to improve data efficiency. (4) ROMBRL demonstrates top performance on both the widely-used D4RL MuJoCo benchmark and a challenging Tokamak Control benchmark for nuclear fusion.

2 Background

Offline Model-based Reinforcement Learning: A Markov Decision Process (MDP) [27] can be described as a tuple $M = \langle \mathcal{S}, \mathcal{A}, P, R, d_0, \gamma \rangle$. \mathcal{S} and \mathcal{A} are the state space and action space, respectively. $P : \mathcal{S} \times \mathcal{A} \rightarrow \Delta_{\mathcal{S}}$ represents the transition dynamics function, $R : \mathcal{S} \times \mathcal{A} \rightarrow \Delta_{[0,1]}$ defines the reward function, and $d_0 : \mathcal{S} \rightarrow \Delta_{\mathcal{S}}$ specifies the initial state distribution, where $\Delta_{\mathcal{X}}$ is the set of probability distributions over the space \mathcal{X} . $\gamma \in [0, 1)$ is a discount factor.

Given an offline dataset of transitions $\mathcal{D}_\mu = \{(s_i, a_i, r_i, s'_i)_{i=1}^N\}$ collected by a behavior policy μ , typical offline MBRL methods first learn a world model P_ϕ, R_ϕ through supervised learning:

$$\max_{\phi} \mathbb{E}_{(s,a,r,s') \sim \mathcal{D}_\mu} [\log P_\phi(s'|s,a) + \log R_\phi(r|s,a)] \quad (1)$$

Then, a policy $\pi_\theta : \mathcal{S} \rightarrow \Delta_{\mathcal{A}}$ is trained to maximize the expected return $J(\theta, \phi)$ in the MDP $M_\phi = \langle \mathcal{S}, \mathcal{A}, P_\phi, R_\phi, d_0, \gamma \rangle$: ($V(s'; \theta, \phi) = \mathbb{E}_{a' \sim \pi_\theta(\cdot|s')} [Q(s', a'|\theta, \phi)]$ is the value function.)

$$\max_{\theta} \mathbb{E}_{s \sim d_0(\cdot), a \sim \pi_\theta(\cdot|s)} [Q(s, a; \theta, \phi)], \quad Q(s, a; \theta, \phi) = \mathbb{E}_{r \sim R_\phi(\cdot|s,a), s' \sim P_\phi(\cdot|s,a)} [r + \gamma V(s'; \theta, \phi)] \quad (2)$$

To address uncertainty of the learned world model, offline MBRL methods [28] usually learn an ensemble of world models from \mathcal{D}_μ and apply an ensemble-based reward penalty to r in Eq. (2), discouraging the agent from exploring regions where predictions from the ensemble members exhibit high variance. However, these reward penalty terms are heuristic-based, and as a result, these algorithms lack formal performance guarantees [29].

Learning Dynamics in Stackelberg Games: In a Stackelberg game, the leader (who plays first) and follower aim to solve the following two optimization problems, respectively:

$$\min_{x_1 \in \mathcal{X}_1} \{f_1(x_1, x_2^*) \mid x_2^* \in \arg \min_{x_2 \in \mathcal{X}_2} f_2(x_1, x_2)\}, \quad \min_{x_2 \in \mathcal{X}_2} f_2(x_1, x_2) \quad (3)$$

The authors of [24] propose update rules for the leader and follower in a class of two-player smooth games defined on continuous and unconstrained $\mathcal{X}_1, \mathcal{X}_2$. Specifically, at each iteration k , x_1 and x_2 are updated as follows:

$$\begin{aligned} x_1^{k+1} &= x_1^k - \eta_1^k \omega_1^k, \quad \omega_1^k = D_1 f_1(x^k) - D_{21} f_2(x^k)^T (D_{22} f_2(x^k))^{-1} D_2 f_1(x^k); \\ x_2^{k+1} &= x_2^k - \eta_2^k \omega_2^k, \quad \omega_2^k = D_2 f_2(x^k). \end{aligned} \quad (4)$$

Here, x^k denotes the value of (x_1, x_2) at iteration k , while (η_1^k, η_2^k) represent the learning rates; $D_1 f_1(x^k)$ represents the partial derivative of $f_1(x^k)$ with respect to x_1 , and similarly for other derivatives. The expression for ω_1^k is derived based on the total derivative of $f_1(x_1, x_2^*)$ with respect to x_1 , of which the details are available in Appendix A.

The learning target for Stackelberg games is to reach Local Stackelberg Equilibrium (LSE [30]):

Definition 1 (LSE). Consider $U_i \subset \mathcal{X}_i$ for each $i \in \{1, 2\}$. The strategy $x_1^* \in U_1$ is a local Stackelberg solution for the leader, if $\forall x_1 \in U_1, \sup_{x_2 \in R_{U_2}(x_1^*)} f_1(x_1^*, x_2) \leq \sup_{x_2 \in R_{U_2}(x_1)} f_1(x_1, x_2)$, where $R_{U_2}(x_1) = \{y \in U_2 \mid f_2(x_1, y) \leq f_2(x_1, x_2), \forall x_2 \in U_2\}$. Moreover, (x_1^*, x_2^*) for any $x_2^* \in R_{U_2}(x_1^*)$ is a Local Stackelberg Equilibrium on $U_1 \times U_2$.

When using unbiased estimators $(\hat{\omega}_1^k, \hat{\omega}_2^k)$ in place of (ω_1^k, ω_2^k) in the iterative updates, Theorem 7 in [24] establishes that there exists a neighborhood $U = U_1 \times U_2$ of the LSE $x^* = (x_1^*, x_2^*)$ such that for any $x^0 \in U$, x^k converges almost surely to x^* . This result holds for a smooth general-sum game (f_1, f_2) , where player 1 is the leader and $\eta_1^k = \mathcal{O}(\eta_2^k)$, under the standard stochastic approximation conditions: $\sum_k \eta_i^k = \infty, \sum_k (\eta_i^k)^2 < \infty, \forall i$.

3 Theoretical Results

Our method is based on an robust offline MBRL objective¹: (For simplicity, we merge P_ϕ and R_ϕ into a single notation, $P_\phi(r, s'|s, a)$, in the following discussion.)

$$\max_{\theta} J(\theta, \phi'), \quad s.t., \quad \phi' \in \arg \min_{\phi \in \Phi} J(\theta, \phi) \quad (5)$$

The uncertainty set $\Phi = \{\phi \in \mathcal{M} \mid \mathbb{E}_{(s,a) \sim \mathcal{D}_\mu, (r,s') \sim P_{\bar{\phi}}(\cdot|s,a)} [\log P_{\bar{\phi}}(r, s'|s, a) - \log P_\phi(r, s'|s, a)] \leq \epsilon\}$, where $\bar{\phi}$ is an optimal solution to Eq. (1) (i.e., a maximum likelihood estimator). **Intuitively, π_θ is trained to maximize its worst-case performance within an uncertainty set of world models, ensuring robust deployment performance.**

¹CPPO-LR, proposed in [20], adopts a similar objective function; however, its theoretical analysis – specifically Lemma 6 and Lemma 7 in its Appendix B.2 – is incorrect.

Define $d_{\theta^*, \phi^*}(s, a) = (1 - \gamma) \sum_{t=0}^{\infty} \gamma^t d_{\theta^*, \phi^*}^t(s, a)$, where θ^* and ϕ^* represent the parameters of a comparator policy and the true MDP, respectively, and $d_{\theta^*, \phi^*}^t(s, a)$ denotes the probability density of the agent reaching (s, a) at time step t when following π_{θ^*} in the environment M_{ϕ^*} . Further, as in [20],

we can define a concentrability coefficient $C_{\phi^*, \theta^*} = \sup_{\phi \in \mathcal{M}} \frac{\mathbb{E}_{(s,a) \sim d_{\theta^*, \phi^*}} [TV(P_{\phi}(\cdot|s, a), P_{\phi^*}(\cdot|s, a))^2]}{\mathbb{E}_{(s,a) \sim d_{\mu, \phi^*}} [TV(P_{\phi}(\cdot|s, a), P_{\phi^*}(\cdot|s, a))^2]}$,

where $TV(\cdot, \cdot)$ denotes the total variation distance between two distributions. Then, we have the following theorem²: (Please refer to Appendix B for the proof.)

Theorem 1. Assume $\phi^* \in \Phi$ with probability at least $1 - \delta/2$. Then, for any comparator policy π_{θ^*} , with probability at least $1 - \delta$, the performance gap in expected return between π_{θ^*} and $\pi_{\hat{\theta}}$ satisfies:

$$J(\theta^*, \phi^*) - J(\hat{\theta}, \phi^*) \leq \frac{\sqrt{C_{\phi^*, \theta^*}}}{(1 - \gamma)^2} \sqrt{4\epsilon + c \left(\sqrt{\frac{\log(2|\Phi|/\delta)}{N}} + \frac{\log(2|\Phi|/\delta)}{N} \right)}, \quad (6)$$

where N and $|\Phi|$ denote the size of \mathcal{D}_{μ} and Φ , respectively, $\hat{\theta}$ is an optimal solution to Eq. (5), and c is a constant.

Notably, if π_{θ^*} is the optimal policy on M_{ϕ^*} and $C_{\phi^*, \theta^*} < \infty$, Eq. (6) represents the suboptimality gap of the learned policy $\pi_{\hat{\theta}}$ through Eq. (5). Moreover, Theorem 1 applies to a general function class of P_{ϕ} and relies on the assumption that $\phi^* \in \Phi$ with probability at least $1 - \delta/2$. By specifying the function class of P_{ϕ} , we can determine the uncertainty range ϵ to ensure that Φ includes ϕ^* with high probability, allowing us to remove this assumption.

Denote \mathcal{D}_{sa}^{μ} as the number of unique state-action pairs in \mathcal{D}_{μ} and N_{sa} as the number of transitions in \mathcal{D}_{μ} that are sampled at (s, a) . Further, we define $\tilde{N} = \max \{N_{sa} \mid (s, a) \in \mathcal{D}_{\mu}\}$. For tabular MDPs, the world models (i.e., P_{ϕ}) follow categorical distributions and we have the following theorem³: (Please refer to Appendix C for the proof and Appendix E for a discussion on $|\Phi|$.)

Theorem 2. In tabular MDPs, suppose K is the alphabet size of the world model and $3 \leq K \leq \frac{N_{sa} C_0}{\epsilon} + 2$, $\forall (s, a) \in \mathcal{D}_{\mu}$. Then, $\phi^* \in \Phi$ with probability at least $1 - \delta/2$ when $\epsilon = \frac{\mathcal{D}_{sa}^{\mu}}{N} \log \frac{2C_1 K (C_0 \tilde{N}/K)^{0.5K} \mathcal{D}_{sa}^{\mu}}{\delta}$.

Further, most recent offline MBRL methods [4, 32, 5] utilize deep neural network-based world models and represent $P_{\phi}(s', r \mid s, a)$ as a multivariate Gaussian distribution with a diagonal covariance matrix, $\forall (s, a)$. In this case, we have the following theorem: (Please check Appendix D for a non-asymptotic representation of ϵ and the proof.)

Theorem 3. For MDPs with continuous state and action spaces, where the world model follows a diagonal Gaussian distribution, let d denote the dimension of the state space. Then, $\phi^* \in \Phi$ with probability at least $1 - \delta/2$, when $\epsilon = \mathcal{O} \left(\frac{\mathcal{D}_{sa}^{\mu} d^2}{N} \log \frac{\mathcal{D}_{sa}^{\mu} d}{\delta} \right)$ as $N_{sa} \rightarrow \infty, \forall (s, a) \in \mathcal{D}_{\mu}$.

4 Policy-guided World Model Adaptation for Enhanced Robustness

To obtain the theoretical guarantee shown in Section 3, the maximin problem in Eq. (5) needs to be well solved. A straightforward approach, as employed in [22], is to update the policy π_{θ} and world model P_{ϕ} alternatively, treating the other as part of the environment during each update step. Specifically, the training process at iteration k is as follows:

$$\theta^{k+1} = \theta^k + \eta_{\theta}^k \nabla_{\theta} J(\theta^k, \phi^k); \quad \phi^{k+1} = \phi^k - \eta_{\phi}^k \nabla_{\phi} \mathcal{L}(\theta^k, \phi^k). \quad (7)$$

Here, $\mathcal{L}(\theta^k, \phi^k) = J(\theta^k, \phi^k) + \lambda \mathbb{E}_{(s,a) \sim \mathcal{D}_{\mu}} [KL(P_{\bar{\phi}}(\cdot|s, a) \parallel P_{\phi^k}(\cdot|s, a)) - \epsilon]$, $\eta_{\theta}^k, \eta_{\phi}^k$ are learning rates at iteration k . In this case, the constrained optimization problem $\min_{\phi \in \Phi} J(\theta, \phi)$ is relaxed into

²For a discounted finite-horizon MDP with horizon h , Theorem 1 remains valid with the following modifications: (1) replacing $\frac{1}{(1-\gamma)^2}$ in Eq. (6) with $\frac{(1-\gamma^h)^2}{(1-\gamma)^2}$ and (2) replacing $d_{\theta^*, \phi^*}(s, a)$ with $d_{\theta^*, \phi^*}^h(s, a) = \frac{1-\gamma}{1-\gamma^h} \sum_{t=0}^h \gamma^t d_{\theta^*, \phi^*}^t(s, a)$. The derivation is similar with the one presented in Appendix B.

³As defined in [31], $C_0 \approx 3.20$ and $C_1 \approx 2.93$. The expression for ϵ when K falls into different ranges (e.g., $K \geq N_{sa} C_0 + 2$) can be derived similarly based on Theorem 3 from [31].

an unconstrained optimization problem $\min_{\phi \in \mathcal{M}} \mathcal{L}(\theta, \phi)$, by employing the Lagrangian formulation and treating the Lagrange multiplier $\lambda > 0$ as a hyperparameter. This method is simple but lacks formal convergence guarantees. The alternating updates may lead to instability due to the non-stationarity introduced by treating the other model as part of the environment in separate updates.

By viewing the policy and world model as the leader and follower in a general-sum Stackelberg game, we can apply the Stackelberg learning dynamics (i.e., Eq. (4)) to iteratively update the policy and world model. Such learning dynamics have proven effective in robust online RL [18] and offline model-free RL [25]. In particular, the update at iteration k is as follows:

$$\begin{aligned}\theta^{k+1} &= \theta^k + \eta_\theta^k [\nabla_\theta J(\theta^k, \phi^k) - \nabla_{\phi\theta}^2 \mathcal{L}(\theta^k, \phi^k)^T (\nabla_\phi^2 \mathcal{L}(\theta^k, \phi^k))^{-1} \nabla_\phi J(\theta^k, \phi^k)]; \\ \phi^{k+1} &= \phi^k - \eta_\phi^k \nabla_\phi \mathcal{L}(\theta^k, \phi^k).\end{aligned}\quad (8)$$

The formula above can be derived by substituting (x_1, x_2) and (f_1, f_2) in Eq. (4) with (θ, ϕ) and $(-J, \mathcal{L})$, respectively. Compared to Eq. (7), the policy updates incorporate gradient information from the world model, as the best-response world model is inherently a function of the policy. This dependency allows the policy optimization process to account for the influence of the evolving world model, leading to potentially more stable learning dynamics. As noted in Section 2, models updated using such learning dynamics are guaranteed to converge to a local Stackelberg equilibrium under mild conditions.

The second approach still solves an unconstrained problem $\min_{\phi \in \mathcal{M}} \mathcal{L}(\theta, \phi)$. As an improvement, we propose a novel learning dynamics, where the follower θ solves the constrained problem $\min_{\phi \in \Phi} J(\theta, \phi)$ as a response to the leader:

$$\begin{aligned}\theta^{k+1} &= \theta^k + \eta_\theta^k [\nabla_\theta J(\theta^k, \phi^k) - \nabla_{\phi\theta}^2 \mathcal{L}(\theta^k, \phi^k, \lambda^k)^T H(\theta^k, \phi^k, \lambda^k) \nabla_\phi J(\theta^k, \phi^k)]; \\ \phi^{k+1} &= \phi^k - \eta_\phi^k \nabla_\phi \mathcal{L}(\theta^k, \phi^k, \lambda^k), \quad \lambda^{k+1} = [\lambda^k + \eta_\lambda^k \nabla_\lambda \mathcal{L}(\theta^k, \phi^k, \lambda^k)]^+.\end{aligned}\quad (9)$$

In the equation above, $H(\theta^k, \phi^k, \lambda^k) = A^{-1} + \lambda^k A^{-1} B S^{-1} B^T A^{-1}$, $S = C - \lambda^k B^T A^{-1} B$, $A = \nabla_\phi^2 \mathcal{L}(\theta^k, \phi^k, \lambda^k)$, $B = \nabla_{\phi\lambda}^2 \mathcal{L}(\theta^k, \phi^k, \lambda^k)$, $C = \nabla_\lambda^2 \mathcal{L}(\theta^k, \phi^k, \lambda^k)$, and $\mathcal{L}(\theta^k, \phi^k, \lambda^k) = J(\theta^k, \phi^k) + \lambda^k \mathbb{E}_{(s,a) \sim \mathcal{D}_\mu} [KL(P_{\tilde{\phi}}(\cdot|s, a) || P_{\phi^k}(\cdot|s, a)) - \epsilon]$ is the Lagrangian. Eq. (9) presents how to update the dual variable in the constrained optimization problem $\min_{\phi \in \Phi} J(\theta, \phi)$, i.e., λ , alongside θ and ϕ . Compared to Eq. (8), the policy updates additionally incorporate gradient information from the best-response dual variable, which is a function of π_θ . This allows the policy optimization to account for the implicit influence of constraint satisfaction, leading to a more informed learning process. The second line in Eq. (9) corresponds to a primal-dual method for solving $\min_{\phi \in \Phi} J(\theta, \phi)$, where $[\cdot]^+$ is a projection operation onto the non-negative real space. Widely used in constrained RL⁴, this method can achieve low suboptimality if the world model's parameterization has sufficient representational capacity, as detailed in [33]. Additionally, the first line in Eq. (9) represents a gradient ascent step corresponding to the objective function $\max_\theta \{J(\theta, \phi^*(\theta)) \mid \phi^*(\theta) \in \arg \min_{\phi \in \Phi} J(\theta, \phi)\}$, of which the derivation is provided in Appendix F. According to the learning dynamics in Stackelberg games and constrained optimization [24, 33], the learning rates in Eq. (9) should satisfy $\eta_\phi^k \gg \eta_\lambda^k \gg \eta_\theta^k$ to ensure convergence.

5 Practical Algorithm: ROMBRL

For a discounted finite-horizon MDP with horizon h , $J(\theta, \phi) = \mathbb{E}_{\tau \sim P(\cdot; \theta, \phi)} \left[\sum_{j=0}^{h-1} \gamma^j r_j \right]$, where $\tau = (s_0, a_0, r_0, \dots, s_h)$ and $P(\tau; \theta, \phi) = d_0(s_0) \prod_{j=0}^{h-1} \pi_\theta(a_j | s_j) P_\phi(r_j, s_{j+1} | s_j, a_j)$. To compute the first-order and second-order derivatives in Eqs. (7) - (9), we have the following theorem:

Theorem 4. For an episodic MDP with horizon h , let $\Psi(\tau, \theta) = \sum_{i=0}^{h-1} \left(\sum_{j=i}^{h-1} \gamma^j r_j \right) \log \pi_\theta(a_i | s_i)$ and $\Psi(\tau, \phi) = \sum_{i=0}^{h-1} \left(\sum_{j=i}^{h-1} \gamma^j r_j \right) \log P_\phi(r_i, s_{i+1} | s_i, a_i)$. Then, we have:

$$\begin{aligned}\nabla_\theta J(\theta, \phi) &= \mathbb{E}_{\tau \sim P(\cdot; \theta, \phi)} [\nabla_\theta \Psi(\tau, \theta)], \quad \nabla_\phi J(\theta, \phi) = \mathbb{E}_{\tau \sim P(\cdot; \theta, \phi)} [\nabla_\phi \Psi(\tau, \phi)], \\ \nabla_{\phi\theta}^2 J(\theta, \phi) &= \mathbb{E}_{\tau \sim P(\cdot; \theta, \phi)} [\nabla_\phi \Psi(\tau, \phi) \nabla_\theta \log P(\tau; \theta, \phi)^T], \\ \nabla_\phi^2 J(\theta, \phi) &= \mathbb{E}_{\tau \sim P(\cdot; \theta, \phi)} [\nabla_\phi \Psi(\tau, \phi) \nabla_\phi \log P(\tau; \theta, \phi)^T + \nabla_\phi^2 \Psi(\tau, \phi)].\end{aligned}\quad (10)$$

⁴Viewing P_ϕ and π_θ as the "policy" and "world model" respectively, $\min_{\phi \in \Phi} J(\theta, \phi)$ is converted into a typical constrained RL problem.

Please refer to Appendix G for the proof of this theorem and the derivatives of $\mathcal{L}(\theta, \phi, \lambda)$.

In a practical algorithm, the expectation terms in Eqs. (10) and (54) are replaced with corresponding unbiased estimators, i.e., the sample means. Estimators of the first-order derivatives can be efficiently computed using automatic differentiation, whose space and time complexity scale linearly with the number of parameters in the models, namely N_θ and N_ϕ . However, computing the second-order derivatives, i.e., $\nabla_\phi^2 \Psi(\pi, \phi)$ in $\nabla_\phi^2 J(\theta, \phi)$ and $\nabla_\phi^2 \log P_\phi$ in $\nabla_\phi^2 \mathcal{L}(\theta, \phi, \lambda)$, can be costly. Instead of substituting the second-order terms with cI as in [34], where I is the identity matrix, we propose the following approximations:

$$\begin{aligned} \mathbb{E}_{\tau \sim P(\cdot; \theta, \phi)} [\nabla_\phi^2 \Psi(\tau, \phi)] &\approx -\mathbb{E}_{\tau \sim P(\cdot; \theta, \phi)} \left[\sum_{i=0}^{h-1} \left(\sum_{j=i}^{h-1} \gamma^j r_j \right) F(s_i, a_i, r_i, s_{i+1}; \phi) \right], \\ \mathbb{E}_{(s, a, r, s') \sim P_\phi \circ \mathcal{D}_\mu(\cdot)} [\nabla_\phi^2 \log P_\phi(r, s' | s, a)] &\approx -\mathbb{E}_{(s, a, r, s') \sim P_\phi \circ \mathcal{D}_\mu(\cdot)} [F(s, a, r, s'; \phi)], \end{aligned} \quad (11)$$

where $F(s, a, r, s'; \phi) = \nabla_\phi \log P_\phi(r, s' | s, a) \nabla_\phi \log P_\phi(r, s' | s, a)^T$ is the Fisher Information Matrix. Thus, we substitute $\nabla_\phi^2 \log P_\phi$ with $-F$, inspired by the fact [35] that $\mathbb{E}_{x \sim P_\phi(\cdot)} [\nabla_\phi^2 \log P_\phi(x) + \nabla_\phi \log P_\phi(x) \nabla_\phi \log P_\phi(x)^T] = 0$. In Appendix H, we discuss the approximation errors that arise when using Eq. (11).

The other computational bottleneck is computing the inverse matrix A^{-1} in Eq. (9)⁵. We choose not to use an identity matrix in place of A^{-1} as done in [13]. As aforementioned, $A = \nabla_\phi^2 \mathcal{L}(\theta, \phi, \lambda)$ is substituted with its sample-based estimator \hat{A} , which is defined as follows:

$$\hat{A} = UV^T - XY^T + ZZ^T, \quad (12)$$

where $U, V \in \mathbb{R}^{N_\phi \times m}$; $X, Y, Z \in \mathbb{R}^{N_\phi \times M}$; m and M represent the number of sampled trajectories and sampled transitions, respectively. Specifically, the i -th columns of U and V are given by $\nabla_\phi \Psi(\tau(i), \phi) / \sqrt{m}$ and $\nabla_\phi \log P(\tau(i); \theta, \phi) / \sqrt{m}$, respectively, where $\tau(i)$ denotes the i -th trajectory sampled from $P(\cdot; \theta, \phi)$. The i -th column of Z is given by $\nabla_\phi \log P_\phi(r_i, s'_i | s_i, a_i) \cdot \sqrt{\lambda/M}$, based on a transition sampled from $P_\phi \circ \mathcal{D}_\mu(\cdot)$. Additionally, by randomly sampling a trajectory τ and a time step $t \sim \text{Uniform}(0, h-1)$, we obtain the columns of X and Y as $\left(\sum_{j=t}^{h-1} \gamma^j r_j \right) \nabla_\phi \log P_\phi(s_{t+1}, r_t | s_t, a_t) \cdot \sqrt{h/M}$ and $\nabla_\phi \log P_\phi(s_{t+1}, r_t | s_t, a_t) \cdot \sqrt{h/M}$, respectively. **Given that $m, M \ll N_\theta, N_\phi$, each term in \hat{A} is a low rank matrix and so we can apply Woodbury matrix identity [24] to efficiently compute \hat{A}^{-1} .**

To summarize, by leveraging Fisher information matrices and the Woodbury matrix identity, we obtain a close approximation of the gradient update for π_θ (i.e., the first line of Eq. (9)), of which the computational complexity scales linearly with the number of parameters in π_θ and P_ϕ . In particular, the time complexity with our design and without it are $\mathcal{O}(mN_\theta + M^2 N_\phi)$ and $\mathcal{O}(mN_\theta + MN_\phi^2 + N_\phi^\omega)$, respectively, where $2 \leq \omega \leq 2.373$. **Please refer to Appendix I for the justification of Eq. (12) and a detailed complexity analysis. The pseudo code and implementation details of our algorithm (ROMBRL) are available in Appendix J.**

6 Experimental Results

In this section, we benchmark our algorithm (ROMBRL) against a range of state-of-the-art (SOTA) offline RL baselines across two task sets comprising a total of 15 continuous control tasks. The first task set is the widely used D4RL MuJoCo suite [36], which includes three types of robotic agents, each with offline datasets of four different quality levels. Since D4RL MuJoCo features deterministic dynamics, we further evaluate on a more challenging set of Tokamak control tasks, where the underlying dynamics are highly stochastic. **To assess the robustness of the policies learned by different algorithms, we introduce noise to the environments' dynamics during deployment. Specifically, at each time step t , the state change (in each dimension) $\Delta s_t = s_{t+1} - s_t$ is perturbed with zero-mean Gaussian noise, where the standard deviation is proportional to Δs_t . In our experiments, we use 5% measurement noise.**

⁵Since S in Eq. (9) is a scalar, its inverse S^{-1} can be easily computed.

Table 1: Comparison of our algorithm with state-of-the-art offline RL methods on the D4RL MuJoCo benchmark. The abbreviations ‘hc’, ‘hp’, and ‘wk’ denote HalfCheetah, Hopper, and Walker2d, respectively. **To evaluate robustness, we introduce measurement noise into the real MuJoCo dynamics.** Each value represents the normalized score, as proposed in [36], of the policy trained by the corresponding algorithm. These scores are undiscounted returns normalized to approximately range between 0 and 100, where a score of 0 corresponds to a random policy and a score of 100 corresponds to an expert-level policy. For each algorithm, we report the average score of the final 100 policy learning epochs and its standard deviation across three random seeds. **The best and second-best results for each task are bolded and marked with * respectively.** The last row includes Cohen’s d to indicate the significance of our algorithm’s improvement over other methods.

Data Type	Agent Type	ROMBRL (ours)	CQL	EDAC	COMBO	RAMBO	MOBILE
random	hc	39.3* (4.0)	18.3 (1.2)	14.9 (7.8)	5.8 (2.1)	36.7 (3.4)	40.3 (2.1)
random	hp	31.3 (0.1)	10.1 (0.4)	14.1 (5.6)	10.3 (3.4)	25.7* (6.1)	22.7 (9.1)
random	wk	21.7 (0.1)	2.3 (1.9)	0.7 (0.3)	0.0 (0.1)	13.1 (3.0)	17.2* (3.3)
medium	hc	77.5* (1.7)	48.5 (0.1)	62.1 (1.0)	49.6 (0.2)	78.1 (1.2)	72.8 (0.5)
medium	hp	102.6 (2.6)	56.1 (0.4)	54.8 (38.4)	71.1 (3.1)	71.7 (8.2)	89.9* (16.1)
medium	wk	79.4* (4.2)	73.9 (0.4)	83.6 (1.4)	72.9 (3.1)	13.7 (5.0)	71.5 (6.1)
med-rep	hc	73.8 (0.4)	45.7 (0.3)	53.2 (0.7)	46.4 (0.2)	65.8 (0.4)	67.6* (4.2)
med-rep	hp	105.3 (0.7)	94.1 (4.7)	101.3 (0.6)	99.5 (1.3)	97.6 (1.1)	104.9* (1.8)
med-rep	wk	90.5 (2.4)	72.2 (17.3)	83.1 (0.3)	71.7 (1.9)	80.9 (1.0)	85.2* (2.3)
med-exp	hc	88.9* (2.1)	88.3 (0.5)	61.2 (6.9)	90.5 (0.0)	83.4 (1.4)	82.9 (5.2)
med-exp	hp	111.9 (0.1)	109.1 (0.9)	55.2 (41.3)	110.1* (0.5)	83.5 (4.9)	79.6 (45.5)
med-exp	wk	110.7* (2.6)	109.9 (0.1)	60.6 (46.3)	37.8 (50.9)	19.5 (20.7)	113.7 (2.5)
Average Score		77.7 (0.5)	60.7 (1.2)	53.7 (4.6)	55.5 (3.6)	55.8 (1.3)	70.7* (2.4)
Cohen’s d		-	18.9	7.4	8.5	22.9	4.1

6.1 Results on D4RL MuJoCo

Here, we compare ROMBRL with several representative offline RL methods, including two model-free algorithms: CQL [2], EDAC [3], and three model-based algorithms: COMBO [29], RAMBO [22], MOBILE [5]. These baselines are carefully selected: EDAC and MOBILE are top model-free and model-based offline RL algorithms on the D4RL Mujoco benchmark, according to [5]; CQL and its model-based extension, COMBO, are widely adopted in real-life robotic tasks; RAMBO is explicitly designed to enhance robustness in offline RL.

In Table 1, we report the convergent performance of each algorithm on all tasks. Following the protocol in the D4RL benchmarking paper [36], convergent performance is defined as the mean evaluation score over the final 100 policy learning epochs. We present the mean (standard deviation) across runs with different random seeds. **ROMBRL ranks first on 7 out of 12 tasks and second on the remaining 5.** In terms of average performance, ROMBRL significantly outperforms all baselines. To quantify the improvement in average performance, we compute Cohen’s d between ROMBRL and each baseline. According to Cohen’s rule of thumb [37], a value of $d \geq 2$ indicates a very large and statistically significant difference. These results demonstrate the superior performance of our algorithm in robust deployment. Additionally, in Figure 2, we present the training curves of each algorithm on all D4RL MuJoCo tasks.

6.2 Results on Tokamak Control

We further evaluate our algorithm on three target tracking tasks for tokamak control. The tokamak is one of the most promising confinement devices for achieving controllable nuclear fusion, where the primary challenge lies in confining the plasma, i.e., an ionized gas of hydrogen isotopes, while heating it and increasing its pressure to initiate and sustain fusion reactions [38]. Tokamak control involves applying a series of direct actuators (e.g., ECH power, magnetic field) and indirect actuators (e.g., setting targets for the plasma shape and density) to confine the plasma to achieve a desired state or track a given target. This sophisticated physical process is an ideal test bed for our algorithm.

As shown in Figure 3, we use a well-trained data-driven dynamics model provided by [39] as a "ground truth" simulator for the nuclear fusion process during evaluation, and generate a dataset

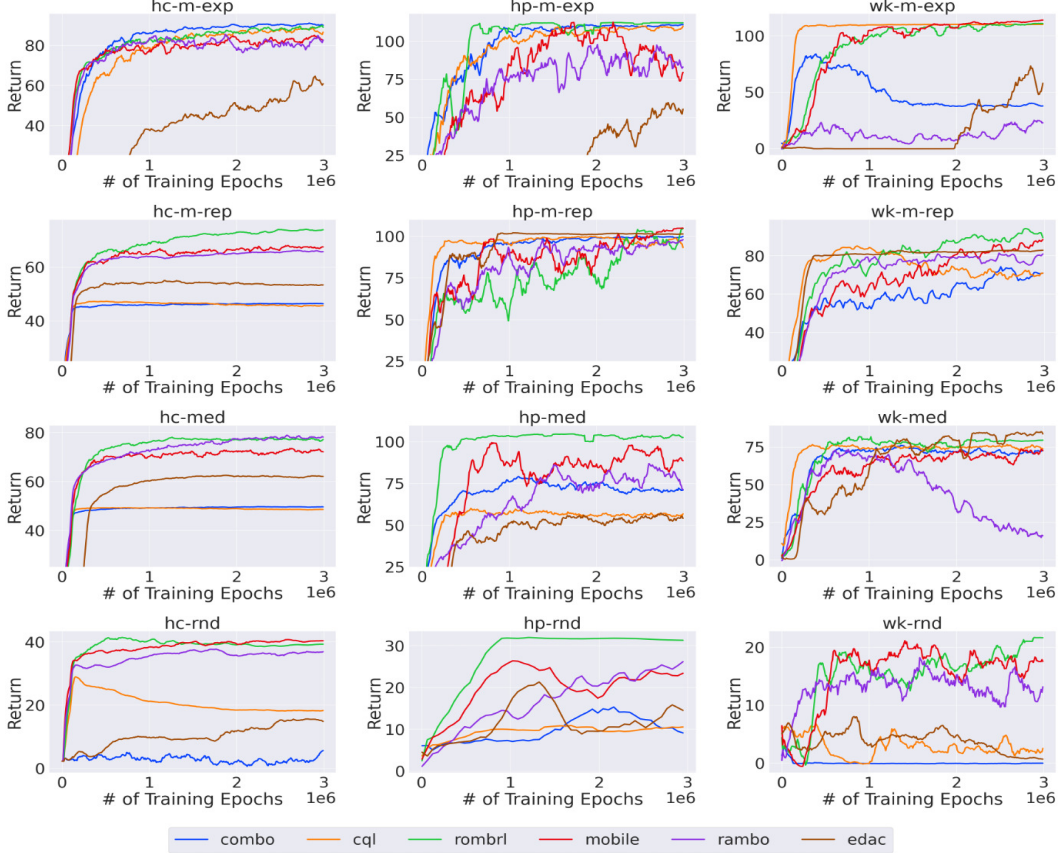


Figure 2: Evaluation results on D4RL MuJoCo. The figure shows the progression of evaluation scores over training epochs for the proposed algorithm and baseline methods. Solid lines indicate the average performance across multiple random seeds. For clarity of presentation, the curves have been smoothed using a sliding window, and confidence intervals are omitted.

containing 111305 transitions for offline RL. We select reference shots (each of which represents a fusion process) from DIII-D⁶, and use trajectories of Ion Rotation, Electron Density, and β_N within them as targets for three tracking tasks. These are critical quantities in tokamak control, particularly β_N , which serves as an economic indicator of the efficiency of nuclear fusion. These continuous control tasks are **highly stochastic**, as the underlying dynamics model is an ensemble of recurrent probabilistic neural networks (RPNNs) and each state transition is a sample from this model. **For details about the simulator, and the design of the state/action spaces and reward functions, please refer to Appendix K.**

In addition to the baselines presented in Table 1, we include a recent model-based offline RL method, BAMCTS [28], which has also been evaluated on Tokamak Control tasks. The benchmarking results are shown in Table 2. The evaluation metric is the negative episodic tracking error of the reference shots, computed as the sum of mean squared errors between the achieved and target quantities at each time step. As in previous experiments, we report the average score over the final 100 policy learning epochs as the policy’s convergent performance. **The results show that ROMBRL ranks first in 2 out of 3 tasks and second in the remaining one.** Moreover, ROMBRL achieves the best average performance across all three tasks, with notably low variance. Cohen’s d further confirms that ROMBRL’s improvement over each baseline is statistically significant. In contrast, the performance of several SOTA model-based methods: RAMBO, MOBILE, and BAMCTS, drops significantly in this stochastic and noisy benchmark, showing poor robustness and high variance across runs. The training curves of each algorithm for all tasks are shown as Figure 4 in Appendix K.

⁶DIII-D is a tokamak device located in San Diego, California, operated by General Atomics.

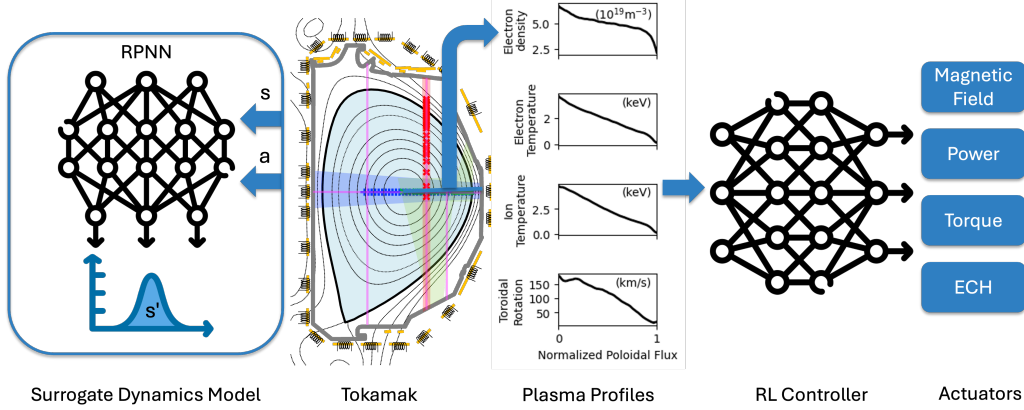


Figure 3: Illustration of the Tokamak Control tasks. The RL controller is trained to apply actuators, such as power and torque, based on the current plasma state, with the goal of driving the plasma toward a target profile. For practical reasons, the real tokamak is replaced with an ensemble of dynamics models trained on operational data from a real device – DIII-D. These models are used to generate data for offline RL and evaluate the trained policies.

Table 2: Comparison of our algorithm with state-of-the-art offline RL methods on the Tokamak Control benchmark. **To evaluate robustness, we inject measurement noise into the tokamak dynamics.** Each value represents the negative episodic tracking error of a specific physical quantity in the reference shot. For each algorithm, we report the average evaluation performance of the final 100 policy learning epochs and its standard deviation across three random seeds. **The best and second-best results for each task are bolded and marked with * respectively.** The last row reports Cohen’s d to quantify the significance of our algorithm’s improvement over competing methods. A value of $d \geq 2$ indicates a statistically significant improvement.

Tracking Target	ROMBRL (ours)	CQL	EDAC	COMBO	RAMBO	MOBILE	BAMCTS
β_N	-70.9* (0.9)	-78.4 (3.1)	-63.4 (1.7)	-84.3 (7.6)	-121.1 (19.9)	-133.9 (10.1)	-111.3 (24.3)
Density	-60.0 (1.9)	-87.3 (12.5)	-112.5 (11.1)	-67.0* (3.1)	-81.3 (15.7)	-75.0 (4.3)	-79.6 (13.8)
Rotation	-10.6 (3.7)	-39.2* (10.1)	-95.4 (44.3)	-69.6 (25.9)	-300.3 (260.5)	-257.6 (153.7)	-305.6 (242.6)
Average Return	-47.1 (1.2)	-68.3* (6.8)	-90.4 (11.5)	-73.6 (5.8)	-167.6 (91.6)	-155.5 (47.7)	-165.5 (84.5)
Cohen’s d	-	4.3	5.3	6.3	1.9	3.2	2.0

7 Conclusion

In this paper, we propose ROMBRL, a novel offline model-based RL algorithm designed to address two key challenges in the field. First, we aim to jointly optimize the world model and policy under a unified objective, thereby resolving the common objective mismatch issue in model-based RL. Second, we focus on enhancing the robustness of the learned policy in adversarial environments – the key to make offline RL applicable to real-world tasks. To this end, we formulate a constrained maximin optimization problem to maximize the worst-case performance of the policy. Specifically, the policy is optimized to maximize its expected return, while the world model is updated adversarially to minimize it. This optimization is carried out using Stackelberg learning dynamics, in which the policy acts as the leader and the world model as the follower, adapting alongside the policy. We provide both theoretical guarantees and efficient training techniques for our algorithm design. ROMBRL is evaluated on multiple adversarial environments, including 12 noisy D4RL MuJoCo tasks and 3 Tokamak Control tasks, covering both deterministic and stochastic dynamics. ROMBRL outperforms a range of SOTA offline RL baselines with statistical significance, demonstrating strong robustness and potential for real-world deployment.

Acknowledgments

This work was funded in part by Department of Energy Fusion Energy Sciences under grant DE-SC0024544.

References

- [1] Levine, S., A. Kumar, G. Tucker, J. Fu. Offline reinforcement learning: Tutorial, review, and perspectives on open problems. *CoRR*, abs/2005.01643, 2020.
- [2] Kumar, A., A. Zhou, G. Tucker, S. Levine. Conservative q-learning for offline reinforcement learning. In *Advances in Neural Information Processing Systems*. 2020.
- [3] An, G., S. Moon, J. Kim, H. O. Song. Uncertainty-based offline reinforcement learning with diversified q-ensemble. In *Advances in Neural Information Processing Systems*, pages 7436–7447. 2021.
- [4] Yu, T., G. Thomas, L. Yu, S. Ermon, J. Y. Zou, S. Levine, C. Finn, T. Ma. MOPO: model-based offline policy optimization. In *Advances in Neural Information Processing Systems*. 2020.
- [5] Sun, Y., J. Zhang, C. Jia, H. Lin, J. Ye, Y. Yu. Model-bellman inconsistency for model-based offline reinforcement learning. In *International Conference on Machine Learning*, vol. 202, pages 33177–33194. PMLR, 2023.
- [6] Chen, J., B. Ganguly, Y. Xu, Y. Mei, T. Lan, V. Aggarwal. Deep generative models for offline policy learning: Tutorial, survey, and perspectives on future directions. *Transactions on Machine Learning Research*, 2024.
- [7] Ross, S., D. Bagnell. Agnostic system identification for model-based reinforcement learning. In *International Conference on Machine Learning*. 2012.
- [8] Hafner, D., T. P. Lillicrap, J. Ba, M. Norouzi. Dream to control: Learning behaviors by latent imagination. In *International Conference on Learning Representations*. 2020.
- [9] Chen, J., V. Aggarwal, T. Lan. A unified algorithm framework for unsupervised discovery of skills based on determinantal point process. In *Advances in Neural Information Processing Systems*. 2023.
- [10] Wei, R., N. Lambert, A. D. McDonald, A. García, R. Calandra. A unified view on solving objective mismatch in model-based reinforcement learning. *Transactions on Machine Learning Research*, 2024, 2024.
- [11] Farahmand, A. Iterative value-aware model learning. In S. Bengio, H. M. Wallach, H. Larochelle, K. Grauman, N. Cesa-Bianchi, R. Garnett, eds., *Advances in Neural Information Processing Systems*, pages 9090–9101. 2018.
- [12] Grimm, C., A. Barreto, S. Singh, D. Silver. The value equivalence principle for model-based reinforcement learning. In *Advances in Neural Information Processing Systems*. 2020.
- [13] Nikishin, E., R. Abachi, R. Agarwal, P. Bacon. Control-oriented model-based reinforcement learning with implicit differentiation. In *AAAI Conference on Artificial Intelligence*, pages 7886–7894. 2022.
- [14] Eysenbach, B., A. Khazatsky, S. Levine, R. Salakhutdinov. Mismatched no more: Joint model-policy optimization for model-based RL. In *Advances in Neural Information Processing Systems*. 2022.
- [15] Ma, Y. J., K. Sivakumar, J. Yan, O. Bastani, D. Jayaraman. Learning policy-aware models for model-based reinforcement learning via transition occupancy matching. In *Learning for Dynamics and Control Conference*, vol. 211, pages 259–271. PMLR, 2023.
- [16] Vemula, A., Y. Song, A. Singh, D. Bagnell, S. Choudhury. The virtues of laziness in model-based RL: A unified objective and algorithms. In *International Conference on Machine Learning*, vol. 202, pages 34978–35005. 2023.
- [17] Yang, S., S. Zhang, Y. Feng, M. Zhou. A unified framework for alternating offline model training and policy learning. In *Advances in Neural Information Processing Systems*. 2022.

- [18] Huang, P., M. Xu, F. Fang, D. Zhao. Robust reinforcement learning as a stackelberg game via adaptively-regularized adversarial training. In *International Joint Conference on Artificial Intelligence*, pages 3099–3106. ijcai.org, 2022.
- [19] Panaganti, K., Z. Xu, D. Kalathil, M. Ghavamzadeh. Robust reinforcement learning using offline data. In *Advances in Neural Information Processing Systems*. 2022.
- [20] Uehara, M., W. Sun. Pessimistic model-based offline reinforcement learning under partial coverage. *CoRR*, abs/2107.06226, 2023.
- [21] Shi, L., Y. Chi. Distributionally robust model-based offline reinforcement learning with near-optimal sample complexity. *Journal of Machine Learning Research*, 25:200:1–200:91, 2024.
- [22] Rigter, M., B. Lacerda, N. Hawes. RAMBO-RL: robust adversarial model-based offline reinforcement learning. In *Advances in Neural Information Processing Systems*. 2022.
- [23] Rajeswaran, A., I. Mordatch, V. Kumar. A game theoretic framework for model based reinforcement learning. In *International Conference on Machine Learning*, vol. 119, pages 7953–7963. PMLR, 2020.
- [24] Fiez, T., B. Chasnov, L. J. Ratliff. Implicit learning dynamics in stackelberg games: Equilibria characterization, convergence analysis, and empirical study. In *International Conference on Machine Learning*, vol. 119 of *Proceedings of Machine Learning Research*, pages 3133–3144. PMLR, 2020.
- [25] Zhou, W., A. Qu. Stackelberg batch policy learning. *CoRR*, abs/2309.16188, 2023.
- [26] Chen, J., T. Lan, V. Aggarwal. Hierarchical deep counterfactual regret minimization. *CoRR*, abs/2305.17327, 2023.
- [27] Puterman, M. L. *Markov decision processes: discrete stochastic dynamic programming*. John Wiley & Sons, 2014.
- [28] Chen, J., W. Chen, J. Schneider. Bayes adaptive monte carlo tree search for offline model-based reinforcement learning. *CoRR*, abs/2410.11234, 2024.
- [29] Yu, T., A. Kumar, R. Rafailov, A. Rajeswaran, S. Levine, C. Finn. COMBO: conservative offline model-based policy optimization. In *Advances in Neural Information Processing Systems*, pages 28954–28967. 2021.
- [30] Başar, T., G. J. Olsder. *Dynamic noncooperative game theory*. Society for Industrial and Applied Mathematics, 1998.
- [31] Mardia, J., J. Jiao, E. Tónczos, R. D. Nowak, T. Weissman. Concentration inequalities for the empirical distribution of discrete distributions: beyond the method of types. *Information and Inference: A Journal of the IMA*, 9(4):813–850, 2020.
- [32] Lu, C., P. J. Ball, J. Parker-Holder, M. A. Osborne, S. J. Roberts. Revisiting design choices in offline model based reinforcement learning. In *International Conference on Learning Representations*. OpenReview.net, 2022.
- [33] Paternain, S., M. Calvo-Fullana, L. F. O. Chamon, A. Ribeiro. Safe policies for reinforcement learning via primal-dual methods. *IEEE Trans. Autom. Control.*, 68(3):1321–1336, 2023.
- [34] Wang, K., S. Shah, H. Chen, A. Perrault, F. Doshi-Velez, M. Tambe. Learning MDPs from features: Predict-then-optimize for sequential decision making by reinforcement learning. In *Advances in Neural Information Processing Systems*. 2021.
- [35] Amari, S.-i. *Information geometry and its applications*, vol. 194. Springer, 2016.
- [36] Fu, J., A. Kumar, O. Nachum, G. Tucker, S. Levine. D4RL: datasets for deep data-driven reinforcement learning. *CoRR*, abs/2004.07219, 2020.
- [37] Sawilowsky, S. S. New effect size rules of thumb. *Journal of modern applied statistical methods*, 8(2):26, 2009.
- [38] Pironti, A., M. Walker. Fusion, tokamaks, and plasma control: an introduction and tutorial. *IEEE Control Systems Magazine*, 25(5):30–43, 2005.
- [39] Char, I., Y. Chung, J. Abbate, E. Kolemen, J. G. Schneider. Full shot predictions for the DIII-D tokamak via deep recurrent networks. *CoRR*, abs/2404.12416, 2024.

- [40] Agarwal, A., S. M. Kakade, A. Krishnamurthy, W. Sun. FLAMBE: structural complexity and representation learning of low rank mdps. In *Advances in Neural Information Processing Systems*. 2020.
- [41] Laurent, B., P. Massart. Adaptive estimation of a quadratic functional by model selection. *Annals of statistics*, pages 1302–1338, 2000.
- [42] Beneventano, P., P. Cheridito, R. Graeber, A. Jentzen, B. Kuckuck. Deep neural network approximation theory for high-dimensional functions. *CoRR*, abs/2112.14523, 2021.
- [43] Shen, G. Exploring the complexity of deep neural networks through functional equivalence. In *International Conference on Machine Learning*. OpenReview.net, 2024.
- [44] Haarnoja, T., A. Zhou, P. Abbeel, S. Levine. Soft actor-critic: Off-policy maximum entropy deep reinforcement learning with a stochastic actor. In *International Conference on Machine Learning*, vol. 80, pages 1856–1865. PMLR, 2018.
- [45] Chen, J., M. Haliem, T. Lan, V. Aggarwal. Multi-agent deep covering skill discovery, 2023.
- [46] Schulman, J., F. Wolski, P. Dhariwal, A. Radford, O. Klimov. Proximal policy optimization algorithms. *CoRR*, abs/1707.06347, 2017.
- [47] Chen, J., B. Ganguly, T. Lan, V. Aggarwal. Variational offline multi-agent skill discovery. *CoRR*, abs/2405.16386, 2024.
- [48] Abbate, J., R. Conlin, E. Kolen. Data-driven profile prediction for diii-d. *Nuclear Fusion*, 61(4):046027, 2021.
- [49] Char, I., J. Abbate, L. Bardoczi, et al. Offline model-based reinforcement learning for tokamak control. In *Learning for Dynamics and Control Conference*, vol. 211, pages 1357–1372. 2023.
- [50] Ariola, M., A. Pironti, et al. *Magnetic control of tokamak plasmas*, vol. 187. Springer, 2008.
- [51] Maćkiewicz, A., W. Ratajczak. Principal components analysis (pca). *Computers & Geosciences*, 19(3):303–342, 1993.

A A Discussion on ω_1^k in Equation (4)

Consider the function $f_1(x_1, x_2^*)$, where $x_2^* \in \arg \min_{x_2 \in \mathcal{X}_2} f_2(x_1, x_2)$ is a function of x_1 . Then, the total derivation of $f_1(x_1, x_2^*)$ with respect to x_1 is given by:

$$Df_1(x_1, x_2^*(x_1)) = \nabla_{x_1} f_1(x_1, x_2^*) + \left(\frac{dx_2^*}{dx_1} \right)^T \nabla_{x_2} f_1(x_1, x_2^*) \quad (13)$$

Since x_2^* is a solution of an unconstrained optimization problem, it satisfies the necessary KKT condition: $\nabla_{x_2} f_2(x_1, x_2^*) = 0$. Thus, $\nabla_{x_2} f_2(x_1, x_2^*)$ is a constant function with respect to x_1 , and we have:

$$\begin{aligned} \frac{d}{dx_1} \nabla_{x_2} f_2(x_1, x_2^*) &= \frac{\partial}{\partial x_1} \nabla_{x_2} f_2(x_1, x_2^*) + \frac{\partial}{\partial x_2} \nabla_{x_2} f_2(x_1, x_2^*) \frac{dx_2^*}{dx_1} \\ &= \nabla_{x_2 x_1}^2 f_2(x_1, x_2^*) + \nabla_{x_2}^2 f_2(x_1, x_2^*) \frac{dx_2^*}{dx_1} = 0, \end{aligned} \quad (14)$$

which implies that $\frac{dx_2^*}{dx_1} = -(\nabla_{x_2}^2 f_2(x_1, x_2^*))^{-1} \nabla_{x_2 x_1}^2 f_2(x_1, x_2^*)$. Plugging this in Eq. (13), we obtain:

$$Df_1(x_1, x_2^*(x_1)) = \nabla_{x_1} f_1(x_1, x_2^*) - \nabla_{x_2 x_1}^2 f_2(x_1, x_2^*)^T (\nabla_{x_2}^2 f_2(x_1, x_2^*))^{-1} \nabla_{x_2} f_1(x_1, x_2^*) \quad (15)$$

By relacing (x_1, x_2^*) with (x_1^k, x_2^k) , we can get ω_1^k in Eq. (4).

B Proof of Theorem 1

We begin our proof by presenting key lemmas. The first one is Lemma 25 from [40].

Lemma 1. *For any two conditional probability densities f_1, f_2 and any distribution $\mathcal{D} \in \Delta_{\mathcal{X}}$, the following inequality holds:*

$$\mathbb{E}_{x \sim \mathcal{D}} [TV(f_1(\cdot|x), f_2(\cdot|x))^2] \leq -2 \log \mathbb{E}_{x \sim \mathcal{D}, y \sim f_2(\cdot|x)} \left[\exp \left(-\frac{1}{2} \log(f_2(y|x)/f_1(y|x)) \right) \right] \quad (16)$$

The second lemma is analogous to the simulation lemma [7] but does not assume knowledge of the reward function.

Lemma 2. *$J(\theta, \phi)$ denotes the expected return of an agent following policy π_θ while interacting with the environment M_ϕ , as defined in Eq. (2). Then, we have:*

$$J(\theta^*, \phi^*) - J(\theta^*, \phi) \leq \frac{1}{(1-\gamma)^2} \mathbb{E}_{(s,a) \sim d_{\theta^*, \phi^*}(\cdot)} [TV(P_{\phi^*}(\cdot|s, a), P_\phi(\cdot|s, a))] \quad (17)$$

Proof.

$$\begin{aligned} &J(\theta^*, \phi^*) - J(\theta^*, \phi) \\ &= \mathbb{E}_{(s,a) \sim \pi_{\theta^*} \circ d_0} \left[\mathbb{E}_{(r,s') \sim P_{\phi^*}} [r + \gamma V(s'; \theta^*, \phi^*)] - \mathbb{E}_{(r,s') \sim P_\phi} [r + \gamma V(s'; \theta^*, \phi)] \right] \\ &= \mathbb{E}_{(s,a) \sim \pi_{\theta^*} \circ d_0} \left[\mathbb{E}_{(r,s') \sim P_{\phi^*}} [r + \gamma V(s'; \theta^*, \phi)] - \mathbb{E}_{(r,s') \sim P_\phi} [r + \gamma V(s'; \theta^*, \phi)] \right] + \\ &\quad \mathbb{E}_{(s,a) \sim \pi_{\theta^*} \circ d_0} \left[\mathbb{E}_{s' \sim P_{\phi^*}} [\gamma V(s'; \theta^*, \phi^*) - \gamma V(s'; \theta^*, \phi)] \right] \\ &= \mathbb{E}_{(s,a) \sim \pi_{\theta^*} \circ d_0} \left[\mathbb{E}_{(r,s') \sim P_{\phi^*}} [r + \gamma V(s'; \theta^*, \phi)] - \mathbb{E}_{(r,s') \sim P_\phi} [r + \gamma V(s'; \theta^*, \phi)] \right] + \\ &\quad \gamma \mathbb{E}_{(s,a) \sim d_{\theta^*, \phi^*}^1} \left[\mathbb{E}_{(r,s') \sim P_{\phi^*}} [r + \gamma V(s'; \theta^*, \phi^*)] - \mathbb{E}_{(r,s') \sim P_\phi} [r + \gamma V(s'; \theta^*, \phi)] \right] \end{aligned} \quad (18)$$

Note that $d_{\theta^*, \phi^*}^0(\cdot) = \pi_{\theta^*} \circ d_0(\cdot)$. By repeatedly applying the process shown above, we obtain:

$$\begin{aligned} &J(\theta^*, \phi^*) - J(\theta^*, \phi) \\ &= \frac{1}{(1-\gamma)} \mathbb{E}_{(s,a) \sim d_{\theta^*, \phi^*}^0} \left[\mathbb{E}_{(r,s') \sim P_{\phi^*}} [r + \gamma V(s'; \theta^*, \phi)] - \mathbb{E}_{(r,s') \sim P_\phi} [r + \gamma V(s'; \theta^*, \phi)] \right] \end{aligned} \quad (19)$$

Now, we analyze the inner term of this expectation:

$$\begin{aligned}
& \mathbb{E}_{(r,s') \sim P_{\phi^*}} [r + \gamma V(s'; \theta^*, \phi)] - \mathbb{E}_{(r,s') \sim P_{\phi}} [r + \gamma V(s'; \theta^*, \phi)] \\
&= \int_{\mathcal{S}, [0,1]} (P_{\phi^*}(r, s'|s, a) - P_{\phi}(r, s'|s, a))(r + \gamma V(s'; \theta^*, \phi) - c) dr ds' \\
&\leq \sup_{r,s'} |r + \gamma V(s'; \theta^*, \phi) - c| \times \int_{\mathcal{S}, [0,1]} |P_{\phi^*}(r, s'|s, a) - P_{\phi}(r, s'|s, a)| dr ds' \\
&\leq \frac{1}{2(1-\gamma)} \int_{\mathcal{S}, [0,1]} |P_{\phi^*}(r, s'|s, a) - P_{\phi}(r, s'|s, a)| dr ds' \\
&= \frac{1}{(1-\gamma)} TV(P_{\phi^*}(\cdot|s, a) - P_{\phi}(\cdot|s, a))
\end{aligned} \tag{20}$$

Here, the second inequality holds if we choose the constant $c = 2/(1-\gamma)$. Combining the two formulas above, we arrive at the final conclusion. \square

Now, we formally begin our proof of Theorem 1:

$$\begin{aligned}
J(\theta^*, \phi^*) - J(\hat{\theta}, \phi^*) &= J(\theta^*, \phi^*) - \min_{\phi \in \Phi} J(\theta^*, \phi) + \min_{\phi \in \Phi} J(\theta^*, \phi) - J(\hat{\theta}, \phi^*) \\
&\leq J(\theta^*, \phi^*) - \min_{\phi \in \Phi} J(\theta^*, \phi) + \min_{\phi \in \Phi} J(\hat{\theta}, \phi) - J(\hat{\theta}, \phi^*)
\end{aligned} \tag{21}$$

This inequality holds because $\hat{\theta}$ is an optimal solution to Eq. (5). Based on the assumption that $\phi^* \in \Phi$ with probability at least $1 - \delta/2$, we have $J(\theta^*, \phi^*) - J(\hat{\theta}, \phi^*) \leq J(\theta^*, \phi^*) - \min_{\phi \in \Phi} J(\theta^*, \phi)$ with probability at least $1 - \delta/2$. Next, we aim to bound $J(\theta^*, \phi^*) - \min_{\phi \in \Phi} J(\theta^*, \phi)$ by establishing an upper bound on $J(\theta^*, \phi^*) - J(\theta^*, \phi)$ for all $\phi \in \Phi$.

Starting from Lemma 2, we have: $(f_{\phi}(s, a) = TV(P_{\phi^*}(\cdot|s, a), P_{\phi}(\cdot|s, a))^2)$

$$\begin{aligned}
& J(\theta^*, \phi^*) - J(\theta^*, \phi) \\
&\leq \frac{1}{(1-\gamma)^2} \mathbb{E}_{(s,a) \sim d_{\theta^*, \phi^*}(\cdot)} [TV(P_{\phi^*}(\cdot|s, a), P_{\phi}(\cdot|s, a))] \\
&\leq \frac{1}{(1-\gamma)^2} \sqrt{\mathbb{E}_{(s,a) \sim d_{\theta^*, \phi^*}(\cdot)} [TV(P_{\phi^*}(\cdot|s, a), P_{\phi}(\cdot|s, a))^2]} \\
&\leq \frac{\sqrt{C_{\phi^*, \theta^*}}}{(1-\gamma)^2} \sqrt{\mathbb{E}_{(s,a) \sim d_{\mu, \phi^*}(\cdot)} [TV(P_{\phi^*}(\cdot|s, a), P_{\phi}(\cdot|s, a))^2]} \\
&= \frac{\sqrt{C_{\phi^*, \theta^*}}}{(1-\gamma)^2} \sqrt{\mathbb{E}_{(s,a) \sim \mathcal{D}_{\mu}} [f_{\phi}(s, a)] + (\mathbb{E}_{(s,a) \sim d_{\mu, \phi^*}(\cdot)} [f_{\phi}(s, a)] - \mathbb{E}_{(s,a) \sim \mathcal{D}_{\mu}} [f_{\phi}(s, a)])^2}
\end{aligned} \tag{22}$$

Next, we bound $\mathbb{E}_{(s,a) \sim \mathcal{D}_{\mu}} [f_{\phi}(s, a)]$ and $\mathbb{E}_{(s,a) \sim d_{\mu, \phi^*}(\cdot)} [f_{\phi}(s, a)] - \mathbb{E}_{(s,a) \sim \mathcal{D}_{\mu}} [f_{\phi}(s, a)]$, separately.

$$\begin{aligned}
& \mathbb{E}_{(s,a) \sim \mathcal{D}_{\mu}} [TV(P_{\phi^*}(\cdot|s, a), P_{\phi}(\cdot|s, a))^2] \\
&\leq 2\mathbb{E}_{(s,a) \sim \mathcal{D}_{\mu}} [TV(P_{\phi^*}(\cdot|s, a), P_{\phi}(\cdot|s, a))^2 + TV(P_{\phi}(\cdot|s, a), P_{\bar{\phi}}(\cdot|s, a))^2]
\end{aligned} \tag{23}$$

According to Lemma 1, we further have:

$$\begin{aligned}
& \mathbb{E}_{(s,a) \sim \mathcal{D}_{\mu}} [TV(P_{\phi}(\cdot|s, a), P_{\bar{\phi}}(\cdot|s, a))^2] \\
&\leq -2 \log \mathbb{E}_{(s,a) \sim \mathcal{D}_{\mu}, (r,s') \sim P_{\bar{\phi}}(\cdot|s, a)} \left[\exp \left(-\frac{1}{2} \log(P_{\bar{\phi}}(r, s'|s, a)/P_{\phi}(r, s'|s, a)) \right) \right] \\
&\leq -2\mathbb{E}_{(s,a) \sim \mathcal{D}_{\mu}, (r,s') \sim P_{\bar{\phi}}(\cdot|s, a)} \left[-\frac{1}{2} \log(P_{\bar{\phi}}(r, s'|s, a)/P_{\phi}(r, s'|s, a)) \right] \\
&= \mathbb{E}_{(s,a) \sim \mathcal{D}_{\mu}, (r,s') \sim P_{\bar{\phi}}(\cdot|s, a)} [\log(P_{\bar{\phi}}(r, s'|s, a)/P_{\phi}(r, s'|s, a))] \leq \epsilon
\end{aligned} \tag{24}$$

Here, the second and third inequalities follow from Jensen's Inequality and the fact that $\phi \in \Phi$. Similarly, since $\phi^* \in \Phi$ with probability at least $1 - \delta/2$, we have $\mathbb{E}_{(s,a) \sim \mathcal{D}_{\mu}} [TV(P_{\phi^*}(\cdot|s, a), P_{\bar{\phi}}(\cdot|s, a))^2] \leq \epsilon$ and so $\mathbb{E}_{(s,a) \sim \mathcal{D}_{\mu}} [TV(P_{\phi^*}(\cdot|s, a), P_{\phi}(\cdot|s, a))^2] \leq 4\epsilon$, with probability at least $1 - \delta/2$.

Finally, we can bound $\mathbb{E}_{(s,a) \sim d_{\mu, \phi^*}(\cdot)} [f_\phi(s, a)] - \mathbb{E}_{(s,a) \sim \mathcal{D}_\mu} [f_\phi(s, a)]$ through the Bernstein's Concentration Inequality, since $\mathbb{E}_{(s,a) \sim \mathcal{D}_\mu} [f_\phi(s, a)]$ is a sample mean, whose expectation is $\mathbb{E}_{(s,a) \sim d_{\mu, \phi^*}(\cdot)} [f_\phi(s, a)]$. Assuming that the state-action pairs in \mathcal{D}_μ are independently sampled from $d_{\mu, \phi^*}(\cdot)$, and using the following properties: $0 \leq f_\phi(s, a) \leq 1$, $|\mathbb{E}_{(s,a) \sim d_{\mu, \phi^*}(\cdot)} [f_\phi(s, a)] - \mathbb{E}_{(s,a) \sim \mathcal{D}_\mu} [f_\phi(s, a)]| \leq 1$, and $\text{Var}_{(s,a) \sim d_{\mu, \phi^*}(\cdot)} (f_\phi(s, a)) \leq \mathbb{E}_{(s,a) \sim d_{\mu, \phi^*}(\cdot)} [f_\phi(s, a)^2] \leq 1$, we have: ($\forall \phi \in \Phi$)

$$\mathbb{E}_{(s,a) \sim d_{\mu, \phi^*}(\cdot)} [f_\phi(s, a)] - \mathbb{E}_{(s,a) \sim \mathcal{D}_\mu} [f_\phi(s, a)] \leq c \left(\sqrt{\frac{\log(2|\Phi|/\delta)}{N}} + \frac{\log(2|\Phi|/\delta)}{N} \right), \quad (25)$$

with probability at least $1 - \delta/2$. Here, we apply Bernstein's Concentration Inequality along with the Union Bound Inequality over the uncertainty set Φ .

To summarize, by applying the Union Bound Inequality to the following events: (1) $\phi^* \in \Phi$ and (2) Eq. (25) holds for all $\phi \in \Phi$, and combining Eqs. (21)-(25), we obtain:

$$J(\theta^*, \phi^*) - J(\hat{\theta}, \phi^*) \leq \frac{\sqrt{C_{\phi^*, \theta^*}}}{(1 - \gamma)^2} \sqrt{4\epsilon + c \left(\sqrt{\frac{\log(2|\Phi|/\delta)}{N}} + \frac{\log(2|\Phi|/\delta)}{N} \right)}, \quad (26)$$

with probability at least $1 - \delta$.

C Proof of Theorem 2

For tabular MDPs, the maximum likelihood estimator $P_{\hat{\phi}}(\cdot|s, a)$ is given by the empirical distribution derived from the samples in \mathcal{D}_μ at each state-action pair (s, a) , i.e., $P_{\hat{\phi}}(\cdot|s, a)$. Thus, we have: $\mathbb{E}_{(s,a) \sim \mathcal{D}_\mu, (r, s') \sim P_{\hat{\phi}}(\cdot|s, a)} [\log P_{\hat{\phi}}(r, s'|s, a) - \log P_{\phi^*}(r, s'|s, a)] = \mathbb{E}_{(s,a) \sim \mathcal{D}_\mu} [KL(P_{\hat{\phi}}(\cdot|s, a) || P_{\phi^*}(\cdot|s, a))]$. According to [31], when $3 \leq K \leq \frac{N_{sa}C_0}{e} + 2$:

$$\mathbb{P}(KL(P_{\hat{\phi}}(\cdot|s, a) || P_{\phi^*}(\cdot|s, a)) \geq \epsilon') \leq C_1 K (C_0 N_{sa}/K)^{0.5K} e^{-N_{sa}\epsilon'}. \quad (27)$$

Setting the right-hand side equal to $\frac{\delta}{2\mathcal{D}_{sa}^\mu}$ and applying the Union Bound Inequality over all $(s, a) \in \mathcal{D}^\mu$, we can obtain that $\mathbb{P}(\cap_{(s,a) \in \mathcal{D}^\mu} X_{sa}) \geq 1 - \delta/2$, where X_{sa} represents the event:

$$KL(P_{\hat{\phi}}(\cdot|s, a) || P_{\phi^*}(\cdot|s, a)) \leq \frac{1}{N_{sa}} \log \frac{2C_1 K (C_0 N_{sa}/K)^{0.5K} \mathcal{D}_{sa}^\mu}{\delta}. \quad (28)$$

Further, $\cap_{(s,a) \in \mathcal{D}^\mu} X_{sa}$ implies:

$$\begin{aligned} \mathbb{E}_{(s,a) \sim \mathcal{D}_\mu} [KL(P_{\hat{\phi}}(\cdot|s, a) || P_{\phi^*}(\cdot|s, a))] &\leq \sum_{(s,a) \sim \mathcal{D}_\mu} \frac{N_{sa}}{N} \frac{1}{N_{sa}} \log \frac{2C_1 K (C_0 N_{sa}/K)^{0.5K} \mathcal{D}_{sa}^\mu}{\delta} \\ &\leq \sum_{(s,a) \sim \mathcal{D}_\mu} \frac{1}{N} \log \frac{2C_1 K (C_0 \tilde{N}/K)^{0.5K} \mathcal{D}_{sa}^\mu}{\delta} \\ &= \frac{\mathcal{D}_{sa}^\mu}{N} \log \frac{2C_1 K (C_0 \tilde{N}/K)^{0.5K} \mathcal{D}_{sa}^\mu}{\delta} = \epsilon \end{aligned} \quad (29)$$

Thus, $\mathbb{P}(\phi^* \in \Phi) = \mathbb{P}(\mathbb{E}_{(s,a) \sim \mathcal{D}_\mu} [KL(P_{\hat{\phi}}(\cdot|s, a) || P_{\phi^*}(\cdot|s, a))] \leq \epsilon) \geq 1 - \delta/2$.

D Proof of Theorem 3

We begin by listing the key lemmas used in the proof. The first lemma is from [41], which claims:

Lemma 3. *Let X be a χ^2 statistic with n degrees of freedom. For any positive t ,*

$$\mathbb{P}(X \leq n - 2\sqrt{nt}) \leq \exp(-t), \quad \mathbb{P}(X \geq n + 2\sqrt{nt} + 2t) \leq \exp(-t). \quad (30)$$

The second lemma establishes a high-probability upper bound on the KL divergence between a univariate Gaussian distribution and its maximum likelihood estimate (MLE).

Lemma 4. Let $\{x_1, \dots, x_n\}$ be independent random samples drawn from a univariate Gaussian distribution $\mathcal{N}(\cdot|\mu, \sigma^2)$. Define $\hat{\mu} = \sum_{i=1}^n x_i/n$ and $\hat{\sigma}^2 = \sum_{i=1}^n (x_i - \hat{\mu})^2/n$. Then, we have $\mathbb{P}(KL(\mathcal{N}(\cdot|\hat{\mu}, \hat{\sigma}^2)||\mathcal{N}(\cdot|\mu, \sigma^2)) \leq \epsilon') \geq 1 - \delta'$, where $\epsilon' = \mathcal{O}\left(\frac{\log(1/\sigma')}{n}\right)$ as $n \rightarrow \infty$.

Proof. Based on the definitions of KL divergence and univariate Gaussian distribution, we have:

$$KL(\mathcal{N}(\cdot|\hat{\mu}, \hat{\sigma}^2)||\mathcal{N}(\cdot|\mu, \sigma^2)) = \frac{1}{2} \left[\frac{\hat{\sigma}^2}{\sigma^2} - \log \frac{\hat{\sigma}^2}{\sigma^2} - 1 + \frac{(\mu - \hat{\mu})^2}{\sigma^2} \right] \quad (31)$$

Let $X_1 = \frac{(\mu - \hat{\mu})^2}{\sigma^2/n}$, then $X_1 \sim \chi_1^2$. According to Lemma 3, $\mathbb{P}(X \geq n + 2\sqrt{nt} + 2t) \leq \exp(-t)$, $\forall t > 0$. Let $\exp(-t) = \frac{\delta'}{2}$, we obtain:

$$\mathbb{P}\left(\frac{(\mu - \hat{\mu})^2}{\sigma^2} \leq \frac{1}{n} \left(1 + 2\sqrt{\log(2/\delta')} + 2\log(2/\delta')\right)\right) \geq 1 - \delta'/2 \quad (32)$$

Further, we observe that $\frac{\hat{\sigma}^2}{\sigma^2} = \frac{\sum_{i=1}^n (x_i - \hat{\mu})^2}{n\sigma^2} = \frac{X_2}{n}$, where $X_2 \sim \chi_{n-1}^2$. Applying the two formulas in Lemma 3 and letting $\exp(-t) = \delta'/4$, we have:

$$\frac{n-1}{n} - 2\sqrt{\frac{(n-1)\log(4/\delta')}{n^2}} \leq \frac{\hat{\sigma}^2}{\sigma^2} \leq \frac{n-1}{n} + 2\sqrt{\frac{(n-1)\log(4/\delta')}{n^2}} + 2\frac{\log(4/\delta')}{n}, \quad (33)$$

with probability at least $1 - \delta'/2$. The continuous function $f(x) = x - \log x - 1$ is monotonically decreasing for $0 < x \leq 1$ and increasing for $x > 1$. Thus, $f\left(\frac{\hat{\sigma}^2}{\sigma^2}\right) \leq \max\{f(x_1), f(x_2)\}$, with probability at least $1 - \delta'/2$, where x_1 and x_2 correspond to the left-hand and right-hand sides of Eq. (33), respectively. Combining this result with Eqs. (31) and (31) and applying the Union Bound Inequality, we obtain:

$$KL(\mathcal{N}(\cdot|\hat{\mu}, \hat{\sigma}^2)||\mathcal{N}(\cdot|\mu, \sigma^2)) \leq \frac{1}{2} \left(\max\{f(x_1), f(x_2)\} + \frac{1}{n} \left(1 + 2\sqrt{\log(2/\delta')} + 2\log(2/\delta')\right) \right), \quad (34)$$

with probability at least $1 - \sigma'$.

Let $x_1 = 1 + t_1$ and $x_2 = 1 + t_2$. Asymptotically, as $n \rightarrow \infty$, $t_1 \rightarrow 0$ and $t_2 \rightarrow 0$. Also, $f(1+t) = \frac{t^2}{2} + \mathcal{O}(t^2)$, as $t \rightarrow 0$. Applying this equation to Eq. (34), we arrive at the conclusion: $\mathbb{P}(KL(\mathcal{N}(\cdot|\hat{\mu}, \hat{\sigma}^2)||\mathcal{N}(\cdot|\mu, \sigma^2)) \leq \epsilon') \geq 1 - \delta'$, where $\epsilon' = \mathcal{O}\left(\frac{\log(1/\sigma')}{n}\right)$ as $n \rightarrow \infty$. \square

For a fixed (s, a) , both $P_{\bar{\phi}}(\cdot | s, a)$ and $P_{\phi^*}(\cdot | s, a)$ define Gaussian distributions with diagonal covariance matrices over a $(d+1)$ -dimensional output space, which consists of the d -dimensional next state and the scalar reward. Thus, each dimension follows a univariate Gaussian distribution and the following equation holds:

$$KL(P_{\bar{\phi}}(\cdot|s, a)||P_{\phi^*}(\cdot|s, a)) = \sum_{i=1}^{d+1} KL(\mathcal{N}(\cdot|\bar{\mu}_{sa}^i, \bar{\sigma}_{sa}^{2,i})||\mathcal{N}(\cdot|\mu_{sa}^i, \sigma_{sa}^{2,i})) \quad (35)$$

Since $P_{\bar{\phi}}$ is an MLE of P_{ϕ^*} , $\bar{\mu}_{sa}^i = \hat{\mu}_{sa}^i$ and $\bar{\sigma}_{sa}^{2,i} = \hat{\sigma}_{sa}^{2,i}$ are the sample mean and sample variance, respectively. Applying Lemma 4 and letting $\delta' = \frac{\delta}{2\mathcal{D}_{sa}^{\mu}(d+1)}$, we obtain:

$$\mathbb{P}(KL(\mathcal{N}(\cdot|\hat{\mu}_{sa}^i, \hat{\sigma}_{sa}^{2,i})||\mathcal{N}(\cdot|\mu_{sa}^i, \sigma_{sa}^{2,i})) \leq \epsilon') \geq 1 - \delta', \quad \epsilon' = \mathcal{O}\left(\frac{d+1}{N_{sa}} \log \frac{2\mathcal{D}_{sa}^{\mu}(d+1)}{\delta}\right) \quad (36)$$

This implies that $\mathbb{P}(KL(P_{\bar{\phi}}(\cdot|s, a)||P_{\phi^*}(\cdot|s, a)) \leq (d+1)\epsilon') \geq 1 - (d+1)\delta'$, based on which we can obtain:

$$\mathbb{E}_{(s,a) \sim \mathcal{D}_{\mu}} [KL(P_{\bar{\phi}}(\cdot|s, a)||P_{\phi^*}(\cdot|s, a))] \leq \sum_{(s,a) \sim \mathcal{D}_{\mu}} \frac{N_{sa}}{N} (d+1)\epsilon' = \epsilon, \quad (37)$$

with probability at least $1 - \delta''$, where $\delta'' = \mathcal{D}_{sa}^{\mu}(d+1)\delta' = \delta/2$ and $\epsilon = \mathcal{O}\left(\frac{\mathcal{D}_{sa}^{\mu}d^2}{N} \log \frac{\mathcal{D}_{sa}^{\mu}d}{\delta}\right)$. A non-asymptotic bound on $\mathbb{E}_{(s,a) \sim \mathcal{D}_{\mu}} [KL(P_{\bar{\phi}}(\cdot|s, a)||P_{\phi^*}(\cdot|s, a))]$ can be similarly derived based on Eq. (34).

E Discussion on the Size of the Function Class

A ξ -cover of a set \mathcal{X} with respect to a metric ρ is a set $\{x_1, \dots, x_n\} \subset \mathcal{X}$ such that for each $x \in \mathcal{X}$, there exists some x_i such that $\rho(x, x_i) \leq \xi$. The ξ -covering number $N(\xi; \mathcal{X}, \rho)$ is the cardinality of the smallest ξ -cover of \mathcal{X} . Based on this definition, we have the following lemma:

Lemma 5. $N(\xi; \mathcal{X}, \|\cdot\|_1) \leq \binom{\lceil \frac{d}{\xi} \rceil + d - 1}{d - 1}$, where $\mathcal{X} = \{x \in \mathbb{R}^d \mid \|x\|_1 = 1, x \succeq 0\}$.

Proof. Let $k = \lceil \frac{d}{\xi} \rceil$ and $\{x_1, \dots, x_n\}$ be the set of all points in \mathcal{X} whose coordinates are integer multiples of $1/k$. The size of this set, i.e., n , corresponds to the number of ways to distribute k units among d coordinates, i.e., $\binom{k+d-1}{d-1}$.

Now, we need to prove that $\forall x \in \mathcal{X}$, there exists some x_i such that $\|x - x_i\|_1 \leq \xi$. Suppose that $g^j \leq x^j \leq g^j + 1/k$, where $j = 1, \dots, d$, g^j are integer multiples of $1/k$, and x^j is the j -th coordinate of x . Then, we have $\sum_{j=1}^d g^j \leq \sum_{j=1}^d x^j = 1 \leq \sum_{j=1}^d g^j + d/k$. This means that we can add m units (each of size $1/k$) to the d coordinates $g^{1:d}$ to construct a valid probability distribution y . Since $0 \leq m \leq d$, y can be constructed to satisfy: $y \in \{x_1, \dots, x_n\}$ and $|y^j - x^j| \leq 1/k, \forall j$, which implies $\|x - y\|_1 \leq d/k \leq \xi$. \square

Next, we show that for tabular MDPs considered in Theorem 2, $J(\theta^*, \phi^*) - J(\hat{\theta}, \hat{\phi}^*) \leq \frac{\sqrt{C_{\phi^*, \theta^*}}}{(1-\gamma)^2} \sqrt{4\epsilon + c' \left(\sqrt{\frac{\log(2N_c/\delta)}{N}} + \frac{\log(2N_c/\delta)}{N} \right)}$, with probability at least $1 - \delta$, where c' is a constant and N_c is upper bounded by $\binom{KN+K-1}{K-1}^{|\mathcal{S}||\mathcal{A}|}$.

Proof. For a fixed (s, a) , $P_\phi(\cdot|s, a) \in \mathbb{R}^K$ is a categorical distribution. According to Lemma 5, the $\frac{1}{N}$ -covering number for $\{P_\phi(\cdot|s, a)\}$ in terms of the L1-norm is upper bounded by $\binom{KN+K-1}{K-1}$. Then, we can construct a set $\{P_1, \dots, P_{N_c}\}$, such that $\forall P_\phi$, there exists P_i such that $\|P_i(\cdot|s, a) - P_\phi(\cdot|s, a)\|_1 \leq \frac{1}{N}$ for all $(s, a) \in \mathcal{S} \times \mathcal{A}$, and we have $N_c \leq \binom{KN+K-1}{K-1}^{|\mathcal{S}||\mathcal{A}|}$.

Repeating the derivation in Appendix B until Eq. (24), we can obtain:

$$J(\theta^*, \phi^*) - J(\hat{\theta}, \hat{\phi}^*) \leq \frac{\sqrt{C_{\phi^*, \theta^*}}}{(1-\gamma)^2} \sqrt{4\epsilon + (\mathbb{E}_{(s,a) \sim d_{\mu, \phi^*}(\cdot)} [f_\phi(s, a)] - \mathbb{E}_{(s,a) \sim \mathcal{D}_\mu} [f_\phi(s, a)]}, \quad (38)$$

with probability at least $1 - \delta/2$, where $f_\phi(s, a) = TV(P_{\phi^*}(\cdot|s, a), P_\phi(\cdot|s, a))^2$. For any P_ϕ and corresponding P_i , we have:

$$\begin{aligned} |f_\phi(s, a) - f_i(s, a)| &= |TV(P_\phi(\cdot|s, a), P_{\phi^*}(\cdot|s, a))^2 - TV(P_i(\cdot|s, a), P_{\phi^*}(\cdot|s, a))^2| \\ &\leq 2|TV(P_\phi(\cdot|s, a), P_{\phi^*}(\cdot|s, a)) - TV(P_i(\cdot|s, a), P_{\phi^*}(\cdot|s, a))| \\ &= \left| \sum_x (|P_\phi(x|s, a) - P_{\phi^*}(x|s, a)| - |P_i(x|s, a) - P_{\phi^*}(x|s, a)|) \right| \\ &\leq \sum_x ||P_\phi(x|s, a) - P_{\phi^*}(x|s, a)| - |P_i(x|s, a) - P_{\phi^*}(x|s, a)|| \\ &\leq \sum_x |P_\phi(x|s, a) - P_i(x|s, a)| \leq 1/N \end{aligned} \quad (39)$$

Here, we apply the difference of squares identity for the first inequality and the triangle inequality for the third inequality. Based on the formula above, we obtain:

$$\begin{aligned} &\mathbb{E}_{(s,a) \sim d_{\mu, \phi^*}(\cdot)} [f_\phi(s, a)] - \mathbb{E}_{(s,a) \sim \mathcal{D}_\mu} [f_\phi(s, a)] \\ &\leq \mathbb{E}_{(s,a) \sim d_{\mu, \phi^*}(\cdot)} [f_i(s, a) + |f_\phi(s, a) - f_i(s, a)|] - \mathbb{E}_{(s,a) \sim \mathcal{D}_\mu} [f_i(s, a) - |f_i(s, a) - f_\phi(s, a)|] \\ &\leq \mathbb{E}_{(s,a) \sim d_{\mu, \phi^*}(\cdot)} [f_i(s, a)] - \mathbb{E}_{(s,a) \sim \mathcal{D}_\mu} [f_i(s, a)] + 2/N \end{aligned} \quad (40)$$

Applying the Bernstein's Concentration Inequality along with the Union Bound Inequality over $\{P_1, \dots, P_{N_c}\}$, we have:

$$\begin{aligned} \mathbb{E}_{(s,a) \sim d_{\mu, \phi^*}(\cdot)} [f_\phi(s, a)] - \mathbb{E}_{(s,a) \sim \mathcal{D}_\mu} [f_\phi(s, a)] &\leq c \left(\sqrt{\frac{\log(2N_c/\delta)}{N}} + \frac{\log(2N_c/\delta)}{N} \right) + \frac{2}{N} \\ &\leq c' \left(\sqrt{\frac{\log(2N_c/\delta)}{N}} + \frac{\log(2N_c/\delta)}{N} \right), \end{aligned} \quad (41)$$

with probability at least $1 - \delta/2$. Thus, we arrive at the conclusion:

$$J(\theta^*, \phi^*) - J(\hat{\theta}, \phi^*) \leq \frac{\sqrt{C_{\phi^*, \theta^*}}}{(1-\gamma)^2} \sqrt{4\epsilon + c' \left(\sqrt{\frac{\log(2N_c/\delta)}{N}} + \frac{\log(2N_c/\delta)}{N} \right)}, \quad (42)$$

with probability at least $1 - \delta$, and $N_c \leq \binom{KN+K-1}{K-1}^{|\mathcal{S}||\mathcal{A}|}$. \square

For MDPs with high-dimensional continuous state and action spaces, it is common practice to learn deep neural network-based world models to ensure that the function space \mathcal{M} adequately represents the true environment MDP and its maximum likelihood estimator [42]. An upper bound on $|\Phi|$ can be similarly derived using the approach outlined above, leveraging bounds on the covering number for deep neural networks [43]. However, as this falls outside the primary focus of this paper – developing a practical algorithm for robust offline MBRL – we leave it as an important direction for future work.

F Derivation of Equation (9)

The derivation process is similar with the one in Appendix A. By substituting (x_1, x_2) and $f_1(x_1, x_2)$ in Eq. (13) with $(\pi, (\frac{\phi}{\lambda}))$ and $-J(\theta, (\frac{\phi}{\lambda})) = -J(\theta, \phi)$ respectively, we obtain the total derivative of $J(\theta, \phi)$ with respect to θ as follows:

$$\begin{aligned} DJ\left(\theta, \left(\frac{\phi}{\lambda}\right)^*(\theta)\right) &= \nabla_\theta J\left(\theta, \left(\frac{\phi}{\lambda}\right)^*(\theta)\right) + \left(\frac{d\phi^*/d\theta}{d\lambda^*/d\theta}\right)^T \nabla_{\left(\frac{\phi}{\lambda}\right)} J\left(\theta, \left(\frac{\phi}{\lambda}\right)^*(\theta)\right) \\ \Rightarrow DJ(\theta, \phi^*(\theta)) &= \nabla_\theta J(\theta, \phi^*) + \left(\frac{d\phi^*/d\theta}{d\lambda^*/d\theta}\right)^T \left(\nabla_{\frac{\phi}{\lambda}} J(\theta, \phi^*)\right) \end{aligned} \quad (43)$$

Here, $(\frac{\phi}{\lambda})^*$ are the optimal primal and dual variables of the constrained problem $\min_{\phi \in \Phi} J(\theta, \phi)$. According to the first-order necessary condition for constrained optimization, we have:

$$\nabla_\phi \mathcal{L}(\theta, \phi^*, \lambda^*) = 0, \quad \lambda^* \nabla_\lambda \mathcal{L}(\theta, \phi^*, \lambda^*) = 0. \quad (44)$$

Here, $\mathcal{L}(\theta, \phi, \lambda) = J(\theta, \phi) + \lambda \mathbb{E}_{(s,a) \sim \mathcal{D}_\mu} [KL(P_{\tilde{\phi}}(\cdot|s, a) || P_\phi(\cdot|s, a))]$ is the Lagrangian and $\nabla_\lambda \mathcal{L}(\theta, \phi, \lambda) = \mathbb{E}_{(s,a) \sim \mathcal{D}_\mu} [KL(P_{\tilde{\phi}}(\cdot|s, a) || P_\phi(\cdot|s, a))]$, so the second condition above corresponds to the complementary slackness. Then, we have:

$$\begin{aligned} \frac{d}{d\theta} (\nabla_\phi \mathcal{L}(\theta, \phi^*, \lambda^*)) &= \nabla_{\phi\theta}^2 \mathcal{L}(\theta, \phi^*, \lambda^*) + \nabla_\phi^2 \mathcal{L}(\theta, \phi^*, \lambda^*) \frac{d\phi^*}{d\theta} + \nabla_{\phi\lambda}^2 \mathcal{L}(\theta, \phi^*, \lambda^*) \frac{d\lambda^*}{d\theta} = 0, \\ \frac{d}{d\theta} (\lambda^* \nabla_\lambda \mathcal{L}(\theta, \phi^*, \lambda^*)) &= \nabla_\lambda \mathcal{L}(\theta, \phi^*, \lambda^*) \frac{d\lambda^*}{d\theta} + \lambda^* \frac{d}{d\theta} (\nabla_\lambda \mathcal{L}(\theta, \phi^*, \lambda^*)) \\ &= \nabla_\lambda \mathcal{L}(\theta, \phi^*, \lambda^*) \frac{d\lambda^*}{d\theta} + \lambda^* \nabla_{\lambda\theta}^2 \mathcal{L}(\theta, \phi^*, \lambda^*) + \\ &\quad \lambda^* \nabla_{\lambda\phi}^2 \mathcal{L}(\theta, \phi^*, \lambda^*) \frac{d\phi^*}{d\theta} + \lambda^* \nabla_\lambda^2 \mathcal{L}(\theta, \phi^*, \lambda^*) \frac{d\lambda^*}{d\theta} = 0 \end{aligned} \quad (45)$$

This implies that $M_1 \left(\frac{d\phi^*/d\theta}{d\lambda^*/d\theta} \right) = -M_2$, where $M_2 = \begin{pmatrix} \nabla_{\phi\theta}^2 \mathcal{L}(\theta, \phi^*, \lambda^*) \\ \lambda^* \nabla_{\lambda\theta}^2 \mathcal{L}(\theta, \phi^*, \lambda^*) \end{pmatrix} = \begin{pmatrix} \nabla_{\phi\theta}^2 \mathcal{L}(\theta, \phi^*, \lambda^*) \\ 0 \end{pmatrix}$ and M_1 is defined as follows:

$$\begin{aligned} M_1 &= \begin{bmatrix} \nabla_\phi^2 \mathcal{L}(\theta, \phi^*, \lambda^*) & \nabla_{\phi\lambda}^2 \mathcal{L}(\theta, \phi^*, \lambda^*) \\ \lambda^* \nabla_{\lambda\phi}^2 \mathcal{L}(\theta, \phi^*, \lambda^*) & \nabla_\lambda \mathcal{L}(\theta, \phi^*, \lambda^*) + \lambda^* \nabla_\lambda^2 \mathcal{L}(\theta, \phi^*, \lambda^*) \end{bmatrix} \\ &= \begin{bmatrix} \nabla_\phi^2 \mathcal{L}(\theta, \phi^*, \lambda^*) & \nabla_{\phi\lambda}^2 \mathcal{L}(\theta, \phi^*, \lambda^*) \\ \lambda^* \nabla_{\lambda\phi}^2 \mathcal{L}(\theta, \phi^*, \lambda^*) & \nabla_\lambda \mathcal{L}(\theta, \phi^*, \lambda^*) \end{bmatrix} = \begin{bmatrix} A & B \\ \lambda^* B^T & C \end{bmatrix} \end{aligned} \quad (46)$$

Assuming A and M_1 are invertible, we have $\left(\frac{d\phi^*/d\theta}{d\lambda^*/d\theta}\right) = -M_1^{-1}M_2$ and further:

$$DJ(\theta, \phi^*(\theta)) = \nabla_{\theta} J(\theta, \phi^*) - M_2^T (M_1^T)^{-1} \left(\nabla_{\phi} J(\theta, \phi^*) \right) \quad (47)$$

Applying the Schur complement of the block A of the matrix M_1^T , i.e., $S = C - \lambda^* B^T A^{-1} B$, we can obtain:

$$(M_1^T)^{-1} = \begin{bmatrix} A^{-1} + \lambda^* A^{-1} B S^{-1} B^T A^{-1} & -\lambda^* A^{-1} B S^{-1} \\ -S^{-1} B^T A^{-1} & S^{-1} \end{bmatrix} \quad (48)$$

$$\Rightarrow DJ(\theta, \phi^*(\theta)) = \nabla_{\theta} J(\theta, \phi^*) - \nabla_{\phi}^2 \mathcal{L}(\theta, \phi^*, \lambda^*)^T H(\theta, \phi^*, \lambda^*) \nabla_{\phi} J(\theta, \phi^*)$$

As in Appendix A and [24], by relacing $(\theta, \phi^*, \lambda^*)$ with $(\theta^k, \phi^k, \lambda^k)$, we obtain the gradient update for θ at iteration k , corresponding to the first line of Eq. (9).

G Proof of Theorem 4

We begin the proof with the definition of the expected return:

$$\begin{aligned} J(\theta, \phi) &= \mathbb{E}_{\tau \sim P(\cdot; \theta, \phi)} \left[\sum_{j=0}^{h-1} \gamma^j r_j \right] = \sum_{j=0}^{h-1} \mathbb{E}_{\tau \sim P(\cdot; \theta, \phi)} [\gamma^j r_j] \\ &= \sum_{j=0}^{h-1} \mathbb{E}_{\tau_j \sim P(\cdot; \theta, \phi)} [\gamma^j r_j] = \sum_{j=0}^{h-1} \int_{T_j} \gamma^j r_j P(\tau_j; \theta, \phi) d\tau_j, \end{aligned} \quad (49)$$

where $\tau_j = (s_0, a_0, r_0, \dots, s_{j+1})$ and the third equality holds because the transitions after step j do not affect the value of r_j and can therefore be marginalized out. Based on this definition, we have:

$$\begin{aligned} \nabla_{\theta} J(\theta, \phi) &= \sum_{j=0}^{h-1} \int_{T_j} \gamma^j r_j \nabla_{\theta} P(\tau_j; \theta, \phi) d\tau_j = \sum_{j=0}^{h-1} \int_{T_j} \gamma^j r_j P(\tau_j; \theta, \phi) \nabla_{\theta} \log P(\tau_j; \theta, \phi) d\tau_j \\ &= \sum_{j=0}^{h-1} \mathbb{E}_{\tau_j \sim P(\cdot; \theta, \phi)} [\gamma^j r_j \nabla_{\theta} \log P(\tau_j; \theta, \phi)] = \mathbb{E}_{\tau \sim P(\cdot; \theta, \phi)} \left[\sum_{j=0}^{h-1} \gamma^j r_j \nabla_{\theta} \log P(\tau_j; \theta, \phi) \right] \\ &= \mathbb{E}_{\tau \sim P(\cdot; \theta, \phi)} \left[\sum_{j=0}^{h-1} \gamma^j r_j \left(\sum_{i=0}^j \nabla_{\theta} \log \pi_{\theta}(a_i | s_i) \right) \right] = \mathbb{E}_{\tau \sim P(\cdot; \theta, \phi)} \left[\sum_{j=0}^{h-1} \sum_{i=0}^j \gamma^j r_j \nabla_{\theta} \log \pi_{\theta}(a_i | s_i) \right] \\ &= \mathbb{E}_{\tau \sim P(\cdot; \theta, \phi)} \left[\sum_{i=0}^{h-1} \sum_{j=i}^{h-1} \gamma^j r_j \nabla_{\theta} \log \pi_{\theta}(a_i | s_i) \right] = \mathbb{E}_{\tau \sim P(\cdot; \theta, \phi)} [\nabla_{\theta} \Psi(\tau, \theta)] \end{aligned} \quad (50)$$

where the second to last equality follows from exchanging the order of summation over the two coordinates. Similarly, we can obtain:

$$\begin{aligned} \nabla_{\phi} J(\theta, \phi) &= \sum_{j=0}^{h-1} \int_{T_j} \gamma^j r_j \nabla_{\phi} P(\tau_j; \theta, \phi) d\tau_j = \sum_{j=0}^{h-1} \int_{T_j} \gamma^j r_j P(\tau_j; \theta, \phi) \nabla_{\phi} \log P(\tau_j; \theta, \phi) d\tau_j \\ &= \sum_{j=0}^{h-1} \mathbb{E}_{\tau_j \sim P(\cdot; \theta, \phi)} [\gamma^j r_j \nabla_{\phi} \log P(\tau_j; \theta, \phi)] = \mathbb{E}_{\tau \sim P(\cdot; \theta, \phi)} \left[\sum_{j=0}^{h-1} \gamma^j r_j \nabla_{\phi} \log P(\tau_j; \theta, \phi) \right] \\ &= \mathbb{E}_{\tau \sim P(\cdot; \theta, \phi)} \left[\sum_{j=0}^{h-1} \sum_{i=0}^j \gamma^j r_j \nabla_{\phi} \log P_{\phi}(r_i, s_{i+1} | s_i, a_i) \right] \\ &= \mathbb{E}_{\tau \sim P(\cdot; \theta, \phi)} \left[\sum_{i=0}^{h-1} \sum_{j=i}^{h-1} \gamma^j r_j \nabla_{\phi} \log P_{\phi}(r_i, s_{i+1} | s_i, a_i) \right] = \mathbb{E}_{\tau \sim P(\cdot; \theta, \phi)} [\nabla_{\phi} \Psi(\tau, \phi)] \end{aligned} \quad (51)$$

Based on the definition of $\nabla_\phi J(\theta, \phi)$, we can get the second-order derivatives as follows:

$$\begin{aligned}
\nabla_\phi^2 J(\theta, \phi) &= \nabla_\phi \mathbb{E}_{\tau \sim P(\cdot; \theta, \phi)} [\nabla_\phi \Psi(\tau, \phi)] = \nabla_\phi \int_T \nabla_\phi \Psi(\tau, \phi) P(\tau; \theta, \phi) d\tau \\
&= \int_T \nabla_\phi^2 \Psi(\tau, \phi) P(\tau; \theta, \phi) + \nabla_\phi \Psi(\tau, \phi) \nabla_\phi P(\tau; \theta, \phi)^T d\tau \\
&= \int_T \nabla_\phi^2 \Psi(\tau, \phi) P(\tau; \theta, \phi) + \nabla_\phi \Psi(\tau, \phi) \nabla_\phi \log P(\tau; \theta, \phi)^T P(\tau; \theta, \phi) d\tau \\
&= \mathbb{E}_{\tau \sim P(\cdot; \theta, \phi)} [\nabla_\phi^2 \Psi(\tau, \phi) + \nabla_\phi \Psi(\tau, \phi) \nabla_\phi \log P(\tau; \theta, \phi)^T]
\end{aligned} \tag{52}$$

$$\begin{aligned}
\nabla_{\phi\theta}^2 J(\theta, \phi) &= \nabla_\theta \mathbb{E}_{\tau \sim P(\cdot; \theta, \phi)} [\nabla_\phi \Psi(\tau, \phi)] = \nabla_\theta \int_T \nabla_\phi \Psi(\tau, \phi) P(\tau; \theta, \phi) d\tau \\
&= \int_T \nabla_{\phi\theta}^2 \Psi(\tau, \phi) P(\tau; \theta, \phi) + \nabla_\phi \Psi(\tau, \phi) \nabla_\theta P(\tau; \theta, \phi)^T d\tau \\
&= \int_T \nabla_{\phi\theta}^2 \Psi(\tau, \phi) P(\tau; \theta, \phi) + \nabla_\phi \Psi(\tau, \phi) \nabla_\theta \log P(\tau; \theta, \phi)^T P(\tau; \theta, \phi) d\tau \\
&= \mathbb{E}_{\tau \sim P(\cdot; \theta, \phi)} [\nabla_{\phi\theta}^2 \Psi(\tau, \phi) + \nabla_\phi \Psi(\tau, \phi) \nabla_\theta \log P(\tau; \theta, \phi)^T] \\
&= \mathbb{E}_{\tau \sim P(\cdot; \theta, \phi)} [\nabla_\phi \Psi(\tau, \phi) \nabla_\theta \log P(\tau; \theta, \phi)^T]
\end{aligned} \tag{53}$$

Here, the last equality holds because $\nabla_\phi \Psi(\tau, \phi)$ is not a function of θ .

Finally, based on Theorem 4 and the definition of $\mathcal{L}(\theta, \phi, \lambda)$ (in Section 4), we can get the following derivatives, which are used in Eqs. (7) - (9):

$$\begin{aligned}
\nabla_\phi \mathcal{L}(\theta, \phi, \lambda) &= \nabla_\phi J(\theta, \phi) - \lambda \mathbb{E}_{(s, a, r, s') \sim P_{\tilde{\phi}} \circ \mathcal{D}_\mu(\cdot)} [\nabla_\phi \log P_\phi(r, s' | s, a)], \\
\nabla_\phi^2 \mathcal{L}(\theta, \phi, \lambda) &= \nabla_\phi^2 J(\theta, \phi) - \lambda \mathbb{E}_{(s, a, r, s') \sim P_{\tilde{\phi}} \circ \mathcal{D}_\mu(\cdot)} [\nabla_\phi^2 \log P_\phi(r, s' | s, a)], \\
\nabla_{\phi\theta}^2 \mathcal{L}(\theta, \phi, \lambda) &= \nabla_{\phi\theta}^2 J(\theta, \phi), \nabla_\lambda \mathcal{L}(\theta, \phi, \lambda) = \mathbb{E}_{(s, a) \sim \mathcal{D}_\mu} [KL(P_{\tilde{\phi}}(\cdot | s, a) || P_\phi(\cdot | s, a)) - \epsilon], \\
\nabla_{\phi\lambda}^2 \mathcal{L}(\theta, \phi, \lambda) &= -\mathbb{E}_{(s, a, r, s') \sim P_{\tilde{\phi}} \circ \mathcal{D}_\mu(\cdot)} [\nabla_\phi \log P_\phi(r, s' | s, a)].
\end{aligned} \tag{54}$$

H Approximation Errors for the Second-Order Derivatives

Firstly, we analyze the approximation error of $\mathbb{E}_{\tau \sim P(\cdot; \theta, \phi)} [\nabla_\phi^2 \Psi(\tau, \phi)]$:

$$\begin{aligned}
&\mathbb{E}_{\tau \sim P(\cdot; \theta, \phi)} [\nabla_\phi^2 \Psi(\tau, \phi)] \\
&= \mathbb{E}_{\tau \sim P(\cdot; \theta, \phi)} \left[\sum_{i=0}^{h-1} \left(\sum_{j=i}^{h-1} \gamma^j r_j \right) \nabla_\phi^2 \log P_\phi(r_i, s_{i+1} | s_i, a_i) \right] \\
&= \mathbb{E}_{\tau \sim P(\cdot; \theta, \phi)} \left[\sum_{i=0}^{h-1} \left(\sum_{j=i}^{h-1} \gamma^j r_j \right) \nabla_\phi \left(\frac{\nabla_\phi P_\phi(r_i, s_{i+1} | s_i, a_i)}{P_\phi(r_i, s_{i+1} | s_i, a_i)} \right) \right] \\
&= \mathbb{E}_{\tau \sim P(\cdot; \theta, \phi)} \left[\sum_{i=0}^{h-1} \left(\sum_{j=i}^{h-1} \gamma^j r_j \right) \left(-\frac{\nabla_\phi P_\phi(r_i, s_{i+1} | s_i, a_i) \nabla_\phi P_\phi(r_i, s_{i+1} | s_i, a_i)^T}{P_\phi(r_i, s_{i+1} | s_i, a_i)^2} \right) \right] + \\
&\quad \mathbb{E}_{\tau \sim P(\cdot; \theta, \phi)} \left[\sum_{i=0}^{h-1} \left(\sum_{j=i}^{h-1} \gamma^j r_j \right) \frac{\nabla_\phi^2 P_\phi(r_i, s_{i+1} | s_i, a_i)}{P_\phi(r_i, s_{i+1} | s_i, a_i)} \right] \\
&= \mathbb{E}_{\tau \sim P(\cdot; \theta, \phi)} \left[\sum_{i=0}^{h-1} \left(\sum_{j=i}^{h-1} \gamma^j r_j \right) \left(-F(s_i, a_i, r_i, s_{i+1}; \phi) + \frac{\nabla_\phi^2 P_\phi(r_i, s_{i+1} | s_i, a_i)}{P_\phi(r_i, s_{i+1} | s_i, a_i)} \right) \right]
\end{aligned} \tag{55}$$

Thus, the approximation error that arise when using Eq. (11) is:

$$\begin{aligned}
& \mathbb{E}_{\tau \sim P(\cdot; \theta, \phi)} \left[\sum_{i=0}^{h-1} \left(\sum_{j=i}^{h-1} \gamma^j r_j \right) \frac{\nabla_\phi^2 P_\phi(r_i, s_{i+1} | s_i, a_i)}{P_\phi(r_i, s_{i+1} | s_i, a_i)} \right] \\
&= \int_T P(\tau; \theta, \phi) \sum_{i=0}^{h-1} \left(\sum_{j=i}^{h-1} \gamma^j r_j \right) \frac{\nabla_\phi^2 P_\phi(r_i, s_{i+1} | s_i, a_i)}{P_\phi(r_i, s_{i+1} | s_i, a_i)} d\tau \\
&= \sum_{i=0}^{h-1} \int_T P(\tau; \theta, \phi) \left(\sum_{j=i}^{h-1} \gamma^j r_j \right) \frac{\nabla_\phi^2 P_\phi(r_i, s_{i+1} | s_i, a_i)}{P_\phi(r_i, s_{i+1} | s_i, a_i)} d\tau \\
&= \sum_{i=0}^{h-1} \int_{T_{i-1} \times \mathcal{A}} P(\tau_{i-1}, a_i; \theta, \phi) d\tau_{i-1} da_i \int_{\mathcal{S} \times [0,1]} \nabla_\phi^2 P_\phi(r_i, s_{i+1} | s_i, a_i) dr_i ds_{i+1} R_i \\
&= \sum_{i=0}^{h-1} \int_{T_{i-1} \times \mathcal{A}} P(\tau_{i-1}, a_i; \theta, \phi) d\tau_{i-1} da_i \nabla_\phi^2 \left(\int_{\mathcal{S} \times [0,1]} P_\phi(r_i, s_{i+1} | s_i, a_i) dr_i ds_{i+1} \right) R_i = 0
\end{aligned} \tag{56}$$

$$\begin{aligned}
& \sum_{i=0}^{h-1} \int_T P(\tau; \theta, \phi) \left(\sum_{j=i+1}^{h-1} \gamma^j r_j \right) \frac{\nabla_\phi^2 P_\phi(r_i, s_{i+1} | s_i, a_i)}{P_\phi(r_i, s_{i+1} | s_i, a_i)} d\tau \\
&= \sum_{i=0}^{h-1} \int_{T_{i-1} \times \mathcal{A}} P(\tau_{i-1}, a_i; \theta, \phi) d\tau_{i-1} da_i \int_{\mathcal{S} \times [0,1]} \nabla_\phi^2 P_\phi(r_i, s_{i+1} | s_i, a_i) dr_i ds_{i+1} R_i \\
&= \sum_{i=0}^{h-1} \int_{T_{i-1} \times \mathcal{A}} P(\tau_{i-1}, a_i; \theta, \phi) d\tau_{i-1} da_i \nabla_\phi^2 \left(\int_{\mathcal{S} \times [0,1]} P_\phi(r_i, s_{i+1} | s_i, a_i) dr_i ds_{i+1} \right) R_i = 0
\end{aligned} \tag{57}$$

Here, $R_i = \int_{T^i} P(\tau^i | \tau_i; \theta, \phi) \left(\sum_{j=i+1}^{h-1} \gamma^j r_j \right) d\tau^i$ and $\tau^i = (a_{i+1}, r_{i+1}, \dots, s_h)$ represents the trajectory segment following τ_i . Combining the two equations above, we have the approximation error as follows:

$$\begin{aligned}
& \mathbb{E}_{\tau \sim P(\cdot; \theta, \phi)} \left[\sum_{i=0}^{h-1} \left(\sum_{j=i}^{h-1} \gamma^j r_j \right) \frac{\nabla_\phi^2 P_\phi(r_i, s_{i+1} | s_i, a_i)}{P_\phi(r_i, s_{i+1} | s_i, a_i)} \right] \\
&= \sum_{i=0}^{h-1} \int_T P(\tau; \theta, \phi) \gamma^i r_i \frac{\nabla_\phi^2 P_\phi(r_i, s_{i+1} | s_i, a_i)}{P_\phi(r_i, s_{i+1} | s_i, a_i)} d\tau \\
&= \sum_{i=0}^{h-1} \int_{T_{i-1} \times \mathcal{A}} P(\tau_{i-1}, a_i; \theta, \phi) d\tau_{i-1} da_i \nabla_\phi^2 \left(\int_{\mathcal{S} \times [0,1]} \gamma^i r_i P_\phi(r_i, s_{i+1} | s_i, a_i) dr_i ds_{i+1} \right) R'_i \\
&= \sum_{i=0}^{h-1} \nabla_\phi^2 \left(\int_{\mathcal{S} \times [0,1]} \gamma^i r_i P_\phi(r_i, s_{i+1} | s_i, a_i) dr_i ds_{i+1} \right),
\end{aligned} \tag{58}$$

where $R'_i = \int_{T^i} P(\tau^i | \tau_i; \theta, \phi) d\tau^i = 1$. Thus, in environments with sparse rewards (where $r(s, a) = 0$ for most (s, a)), the approximation error of $\mathbb{E}_{\tau \sim P(\cdot; \theta, \phi)} \left[\nabla_\phi^2 \Psi(\tau, \phi) \right]$ can be negligible.

Secondly, we analyze the approximation error of $\mathbb{E}_{(s,a,r,s') \sim P_{\bar{\phi}} \circ \mathcal{D}_\mu(\cdot)} \left[\nabla_\phi^2 \log P_\phi(r, s' | s, a) \right]$:

$$\begin{aligned}
& \mathbb{E}_{(s,a,r,s') \sim P_{\bar{\phi}} \circ \mathcal{D}_\mu(\cdot)} \left[\nabla_\phi^2 \log P_\phi(r, s' | s, a) \right] \\
&= \mathbb{E}_{(s,a,r,s') \sim P_{\bar{\phi}} \circ \mathcal{D}_\mu(\cdot)} \left[\nabla_\phi \left(\frac{\nabla_\phi P_\phi(r, s' | s, a)}{P_\phi(r, s' | s, a)} \right) \right] \\
&= \mathbb{E}_{(s,a,r,s') \sim P_{\bar{\phi}} \circ \mathcal{D}_\mu(\cdot)} \left[-\frac{\nabla_\phi P_\phi(r, s' | s, a) \nabla_\phi P_\phi(r, s' | s, a)^T}{P_\phi(r, s' | s, a)^2} + \frac{\nabla_\phi^2 P_\phi(r, s' | s, a)}{P_\phi(r, s' | s, a)} \right] \\
&= \mathbb{E}_{(s,a,r,s') \sim P_{\bar{\phi}} \circ \mathcal{D}_\mu(\cdot)} \left[-F(s, a, r, s'; \phi) + \frac{\nabla_\phi^2 P_\phi(r, s' | s, a)}{P_\phi(r, s' | s, a)} \right]
\end{aligned} \tag{59}$$

Thus, the approximation error is:

$$\begin{aligned} & \mathbb{E}_{(s,a,r,s') \sim P_{\bar{\phi}} \circ \mathcal{D}_{\mu}(\cdot)} \left[\frac{\nabla_{\phi}^2 P_{\phi}(r, s' | s, a)}{P_{\phi}(r, s' | s, a)} \right] \\ &= \mathbb{E}_{(s,a) \sim \mathcal{D}_{\mu}(\cdot)} \left[\int_{S \times [0,1]} P_{\bar{\phi}}(r, s' | s, a) \frac{\nabla_{\phi}^2 P_{\phi}(r, s' | s, a)}{P_{\phi}(r, s' | s, a)} dr ds' \right], \end{aligned} \quad (60)$$

which equals 0 if $P_{\bar{\phi}} = P_{\phi}$. This holds approximately since P_{ϕ} is constrained to remain close to $P_{\bar{\phi}}$.

I Analysis of Time Complexity

First, we justify the sample-based estimator of $A = \nabla_{\phi}^2 \mathcal{L}(\theta, \phi, \lambda)$, as given in Eq. (12). According to Eqs. (10), (54), and (11), $\mathcal{L}(\theta, \phi, \lambda)$ can be approximated as follows:

$$\begin{aligned} \nabla_{\phi}^2 \mathcal{L}(\theta, \phi, \lambda) &= \mathbb{E}_{\tau \sim P(\cdot; \theta, \phi)} \left[\nabla_{\phi} \Psi(\tau, \phi) \nabla_{\phi} \log P(\tau; \theta, \phi)^T + \nabla_{\phi}^2 \Psi(\tau, \phi) \right] \\ &\quad - \lambda \mathbb{E}_{(s,a,r,s') \sim P_{\bar{\phi}} \circ \mathcal{D}_{\mu}(\cdot)} \left[\nabla_{\phi}^2 \log P_{\phi}(r, s' | s, a) \right] \\ &\approx \mathbb{E}_{\tau \sim P(\cdot; \theta, \phi)} \left[\nabla_{\phi} \Psi(\tau, \phi) \nabla_{\phi} \log P(\tau; \theta, \phi)^T - \sum_{i=0}^{h-1} \left(\sum_{j=i}^{h-1} \gamma^j r_j \right) F(s_i, a_i, r_i, s_{i+1}; \phi) \right] \\ &\quad + \lambda \mathbb{E}_{(s,a,r,s') \sim P_{\bar{\phi}} \circ \mathcal{D}_{\mu}(\cdot)} \left[F(s, a, r, s'; \phi) \right] \end{aligned} \quad (61)$$

where $F(s, a, r, s'; \phi) = \nabla_{\phi} \log P_{\phi}(r, s' | s, a) \nabla_{\phi} \log P_{\phi}(r, s' | s, a)^T$. Then, we can apply unbiased estimators for each of the three terms in Eq. (61):

$$\begin{aligned} & \mathbb{E}_{\tau \sim P(\cdot; \theta, \phi)} \left[\nabla_{\phi} \Psi(\tau, \phi) \nabla_{\phi} \log P(\tau; \theta, \phi)^T \right] \\ &\approx \frac{1}{m} \sum_{i=1}^m \nabla_{\phi} \Psi(\tau(i), \phi) \nabla_{\phi} \log P(\tau(i); \theta, \phi)^T = UV^T, \\ & \lambda \mathbb{E}_{(s,a,r,s') \sim P_{\bar{\phi}} \circ \mathcal{D}_{\mu}(\cdot)} \left[F(s, a, r, s'; \phi) \right] \\ &\approx \frac{\lambda}{M} \sum_{i=1}^M \nabla_{\phi} \log P_{\phi}(r_i, s'_i | s_i, a_i) \nabla_{\phi} \log P_{\phi}(r_i, s'_i | s_i, a_i)^T = ZZ^T, \\ & \mathbb{E}_{\tau \sim P(\cdot; \theta, \phi)} \left[\sum_{i=0}^{h-1} \left(\sum_{j=i}^{h-1} \gamma^j r_j \right) F(s_i, a_i, r_i, s_{i+1}; \phi) \right] \\ &= \sum_{t=0}^{h-1} \mathbb{E}_{\tau \sim P(\cdot; \theta, \phi)} \left[\left(\sum_{j=t}^{h-1} \gamma^j r_j \right) F(s_t, a_t, r_t, s_{t+1}; \phi) \right] \\ &= h \mathbb{E}_{t \sim \text{Uniform}(0, h-1), \tau \sim P(\cdot; \theta, \phi)} \left[\left(\sum_{j=t}^{h-1} \gamma^j r_j \right) F(s_t, a_t, r_t, s_{t+1}; \phi) \right] \approx XY^T. \end{aligned} \quad (62)$$

Thus, $\hat{A} = UV^T - XY^T + ZZ^T$ is an unbiased estimator of the Fisher-information-matrix-based approximation of $\nabla_{\phi}^2 \mathcal{L}(\theta, \phi, \lambda)$, where $U, V \in \mathbb{R}^{N_{\phi} \times m}$; $X, Y, Z \in \mathbb{R}^{N_{\phi} \times M}$; m and M represent the number of sampled trajectories and sampled transitions, respectively. Please check Section 5 for the definitions of U, V, X, Y, Z . Similarly, we can obtain the unbiased estimator of $\nabla_{\phi\theta}^2 \mathcal{L}(\theta, \phi, \lambda)$:

$$\begin{aligned} \nabla_{\phi\theta}^2 \mathcal{L}(\theta, \phi, \lambda) &= \nabla_{\phi\theta}^2 J(\theta, \phi) = \mathbb{E}_{\tau \sim P(\cdot; \theta, \phi)} \left[\nabla_{\phi} \Psi(\tau, \phi) \nabla_{\theta} \log P(\tau; \theta, \phi)^T \right] \\ &\approx \frac{1}{m} \sum_{i=1}^m \nabla_{\phi} \Psi(\tau(i), \phi) \nabla_{\theta} \log P(\tau(i); \theta, \phi)^T = UW^T, \end{aligned} \quad (63)$$

where $W \in \mathbb{R}^{N_{\theta} \times m}$ and the i -th column of W is $\nabla_{\theta} \log P(\tau(i); \theta, \phi)$.

Next, we analyze the time complexity of estimating the total derivative in Eq. (9), i.e., $\nabla_{\theta} J(\theta, \phi) - \nabla_{\phi\theta}^2 \mathcal{L}(\theta, \phi, \lambda)^T H(\theta, \phi, \lambda) \nabla_{\phi} J(\theta, \phi)$ without applying the Woodbury matrix identity to invert \hat{A} . We note that (1) $H(\theta, \phi, \lambda) = A^{-1} + \lambda A^{-1} B S^{-1} B^T A^{-1}$, $S = C - \lambda B^T A^{-1} B$, $B = \nabla_{\phi\lambda}^2 \mathcal{L}(\theta, \phi, \lambda)$, $C = \nabla_{\lambda} \mathcal{L}(\theta, \phi, \lambda)$; (2) sample-based (unbiased) estimators $\hat{A}, \hat{B}, \hat{C}, \nabla_{\theta} \hat{J}(\theta, \phi), \nabla_{\phi} \hat{J}(\theta, \phi)$ are used in place of the corresponding expectation terms; (3) we analyze the time complexity after getting $\hat{B}, \hat{C}, \nabla_{\theta} \hat{J}(\theta, \phi), \nabla_{\phi} \hat{J}(\theta, \phi), U, V, W, X, Y, Z$, since computing these quantities is unavoidable and the computational cost of these terms only scales linearly with N_{θ} and N_{ϕ} ; (4) As a common practice, \hat{A} is computed as $UV^T - XY^T + ZZ^T + cI$ to ensure its invertibility.

The time complexity of multiplying a $p \times k$ matrix with a $k \times q$ matrix is $\mathcal{O}(pkq)$, while the complexity of inverting a $p \times p$ matrix is $\mathcal{O}(p^{\omega})$, where ω ranges from 2 to approximately 2.373. **Denote $TC(\cdot)$ as the time complexity of computing a certain term based on existing terms.** Then, $TC(\hat{A}) = \mathcal{O}(mN_{\phi}^2 + MN_{\phi}^2)$, $TC(\hat{A}^{-1}) = \mathcal{O}(N_{\phi}^{\omega})$, $TC(\hat{S}) = \mathcal{O}(N_{\phi}^2)$, $TC(\hat{S}^{-1}) = \mathcal{O}(1)$. With $\hat{A}^{-1}, \hat{B}, \hat{S}^{-1}, \nabla_{\phi} \hat{J}(\theta, \phi)$, we can compute $M_1 = \hat{H}(\theta, \phi, \lambda) \nabla_{\phi} \hat{J}(\theta, \phi)$ by recursively performing matrix multiplications from right to left. Thus, we have $TC(M_1) = \mathcal{O}(N_{\phi}^2)$, and similarly, $TC(WU^T M_1) = \mathcal{O}(mN_{\phi} + mN_{\theta})$. **To sum up, the time complexity to get an estimate of $\nabla_{\theta} J(\theta, \phi) - \nabla_{\phi\theta}^2 \mathcal{L}(\theta, \phi, \lambda)^T H(\theta, \phi, \lambda) \nabla_{\phi} J(\theta, \phi)$ without applying the Woodbury matrix identity is $\mathcal{O}(MN_{\phi}^2 + N_{\phi}^{\omega} + mN_{\theta})$.**

Last, we introduce how to calculate \hat{A}^{-1} by recursively applying the Woodbury matrix identity and how it can decrease the time complexity. To be specific, we have:

$$\begin{aligned} \hat{A}^{-1} &= (UV^T + ZZ^T - XY^T + cI)^{-1} = (M_2 + UV^T)^{-1} \\ &= M_2^{-1} - M_2^{-1}U(I + V^T M_2^{-1}U)^{-1}V^T M_2^{-1}, \end{aligned} \quad (64)$$

where the last equality is the direct result of applying the Woodbury matrix identity⁷. Repeating such a process, we can obtain:

$$\begin{aligned} M_2^{-1} &= (ZZ^T - XY^T + cI)^{-1} = (M_3 + ZZ^T)^{-1} \\ &= M_3^{-1} - M_3^{-1}Z(I + Z^T M_3^{-1}Z)^{-1}Z^T M_3^{-1}, \\ M_3^{-1} &= (cI - XY^T)^{-1} = \frac{1}{c}I + \frac{1}{c}X(I - \frac{1}{c}Y^T X)^{-1} \left(\frac{1}{c}Y^T \right) \\ &= \frac{1}{c}I + \frac{1}{c}X(cI - Y^T X)^{-1}Y^T. \end{aligned} \quad (65)$$

Note that we do not compute or store \hat{A}^{-1} . Instead, we directly compute the the multiplication of \hat{A}^{-1} with another matrix. For example, to compute $\hat{A}^{-1}\hat{B}$, we need to compute $M_2^{-1}\hat{B}$ and $M_2^{-1}U$, and $TC(M_2^{-1}\hat{B})$ is dominated by $TC(M_2^{-1}U)$. Then, to compute $M_2^{-1}U$, we need $M_3^{-1}U$ and $M_3^{-1}Z$, and $TC(M_3^{-1}U)$ is dominated by $TC(M_3^{-1}Z)$. We can calculate $M_3^{-1}Z = \frac{1}{c}Z + \frac{1}{c}X(cI - Y^T X)^{-1}Y^T Z$ by first computing $(cI - Y^T X)^{-1}$ and then recursively performing matrix multiplications from right to left, so $TC(M_3^{-1}Z) = \mathcal{O}(M^2 N_{\phi} + M^3)$. With $M_3^{-1}Z$ and $M_3^{-1}U$, we can compute $M_2^{-1}U$. Still by recursively performing matrix multiplications from right to left, we get $TC(M_2^{-1}U) = \mathcal{O}(M^2 N_{\phi} + M^2 m)$. Finally, we can get $\hat{A}^{-1}\hat{B}$ based on $M_2^{-1}U$ and $M_2^{-1}\hat{B}$ with a time complexity of $\mathcal{O}(m^2 N_{\phi})$. **To sum up, the entire process of computing $\hat{A}^{-1}\hat{B}$ requires $\mathcal{O}(M^2 N_{\phi})$ time.**

Similarly, the time complexity of computing $\hat{A}^{-1}\nabla_{\phi} \hat{J}(\theta, \phi)$ is also $\mathcal{O}(M^2 N_{\phi})$. Given $\hat{A}^{-1}\hat{B}$, $TC(\hat{S}) = \mathcal{O}(N_{\phi})$ and $TC(\hat{S}^{-1}) = \mathcal{O}(1)$. With $\hat{A}^{-1}\hat{B}$, $\hat{A}^{-1}\nabla_{\phi} \hat{J}(\theta, \phi)$, and \hat{S}^{-1} , we can compute $M_1 = \hat{H}(\theta, \phi, \lambda) \nabla_{\phi} \hat{J}(\theta, \phi) = \hat{A}^{-1}\nabla_{\phi} \hat{J}(\theta, \phi) + \lambda \hat{A}^{-1}\hat{B}\hat{S}^{-1}\hat{B}^T \hat{A}^{-1}\nabla_{\phi} \hat{J}(\theta, \phi)$ by recursively performing matrix multiplications from right to left, thus $TC(M_1) = \mathcal{O}(N_{\phi})$. Finally, we have $TC(WU^T M_1) = \mathcal{O}(mN_{\phi} + mN_{\theta})$, and **the overall time complexity to get an estimate of**

⁷The Woodbury matrix identity states that $(A + UCV)^{-1} = A^{-1} - A^{-1}U(C^{-1} + VA^{-1}U)^{-1}VA^{-1}$, where A is $n \times n$, C is $k \times k$, U is $n \times k$, and V is $k \times n$. The notations used here are independent of those in the main content.

Algorithm 1 Vanilla ROMBRL

- 1: **Input:** offline dataset \mathcal{D}_μ , learning rates $\eta_\theta, \eta_\phi, \eta_\lambda$ with $\eta_\phi \gg \eta_\lambda \gg \eta_\theta$, # of training iterations K , uncertainty range ϵ
 - 2: Obtain $\bar{\phi} \in \arg \max_\phi \mathbb{E}_{(s,a,r,s') \sim \mathcal{D}_\mu} [\log P_\phi(s', r|s, a)]$
 - 3: Initialize θ^1, ϕ^1 , and λ^1 with $\lambda^1 > 0$
 - 4: **for** $k = 1 \dots K$ **do**
 - 5: Sample trajectories from $P(\cdot; \theta^k, \phi^k)$ and state transitions from $P_{\bar{\phi}} \circ \mathcal{D}_\mu(\cdot)$
 - 6: $\theta^{k+1} \leftarrow \theta^k + \eta_\theta [\nabla_\theta \hat{J}(\theta^k, \phi^k) - \nabla_{\phi\theta}^2 \hat{\mathcal{L}}(\theta^k, \phi^k, \lambda^k)^T \hat{H}(\theta^k, \phi^k, \lambda^k) \nabla_\phi \hat{J}(\theta^k, \phi^k)]$
 - 7: $\phi^{k+1} \leftarrow \phi^k - \eta_\phi \nabla_\phi \hat{\mathcal{L}}(\theta^k, \phi^k, \lambda^k)$
 - 8: $\lambda^{k+1} \leftarrow [\lambda^k + \eta_\lambda \nabla_\lambda \hat{\mathcal{L}}(\theta^k, \phi^k, \lambda^k)]^+$
 - 9: **end for**
-

$\nabla_\theta J(\theta, \phi) - \nabla_{\phi\theta}^2 \mathcal{L}(\theta, \phi, \lambda)^T H(\theta, \phi, \lambda) \nabla_\phi J(\theta, \phi)$ when applying the Woodbury matrix identity is $\mathcal{O}(M^2 N_\phi + m N_\theta)$, which is linear with the number of parameters in the policy and world model.

J Algorithm Details

In this section, we first present the pseudo code of a vanilla version of our algorithm, as a summary of Sections 4 and 5. Then, we introduce modifications in the actual implementation, for improved sample efficiency and training stability.

In Algorithm 1, Lines 6 – 8 correspond to the learning dynamics in Eq. (9), where $\hat{H}(\theta^k, \phi^k, \lambda^k) = \hat{A}^{-1} + \lambda^k \hat{A}^{-1} \hat{B} \hat{S}^{-1} \hat{B}^T \hat{A}^{-1}$, $\hat{S} = \hat{C} - \lambda^k \hat{B}^T \hat{A}^{-1} \hat{B}$, $\hat{A} = \nabla_\phi^2 \hat{\mathcal{L}}(\theta^k, \phi^k, \lambda^k)$, $\hat{B} = \nabla_{\phi\lambda}^2 \hat{\mathcal{L}}(\theta^k, \phi^k, \lambda^k)$, $\hat{C} = \nabla_\lambda \hat{\mathcal{L}}(\theta^k, \phi^k, \lambda^k)$. As a common practice, we use sample-based (unbiased) estimators in place of corresponding expectation terms. The definitions of these terms are available in Eqs. (10), (11), and (54). Additionally, Eqs. (64) and (65) present how to efficiently compute \hat{A}^{-1} using the Woodbury matrix identity.

Algorithm 1 differs from typical offline MBRL algorithms, such as [5, 28], in several key aspects. **First**, they learn an ensemble of world models through supervised learning before the MBRL process, as in Line 2 of Algorithm 1. However, unlike our approach, the world models are not updated alongside the policy during MBRL. **Second**, they introduce an additional penalty term to the predicted reward from $P_{\bar{\phi}}$. This penalty is large when there is high variance among the predictions from different ensemble members, discouraging the agent from visiting uncertain regions in the state-action space. **Third**, at each training iteration, they randomly sample a set of states from \mathcal{D}_μ as starting points for imaginary rollouts. During these rollouts, the policy π_θ interacts with $P_{\bar{\phi}}$ for a short horizon of length l , collecting transitions into a replay buffer for RL. The use of short-horizon rollouts helps mitigate compounding errors caused by inaccurate world model predictions. Finally, they train π_θ for multiple epochs using transitions stored in the buffer with Soft Actor-Critic (SAC) [44, 45], an off-policy RL algorithm.

In Algorithm 1, we propose a co-training scheme for the policy and world model to enhance robustness, addressing uncertainties arising from inaccurate world model predictions or insufficient coverage of \mathcal{D}_μ . This approach serves as an alternative to using a world model ensemble and ensemble-based reward penalties, which lack strong theoretical justification. However, as noted in the third point above, off-policy training can improve sample efficiency, and short-horizon rollouts are generally preferred in model-based RL to mitigate compounding errors. **In this case, we propose several modifications to Algorithm 1 to enhance its empirical performance, resulting in Algorithm 2.**

Given that the underlying world model is continuously updated, maintaining a large replay buffer and computing policy gradients based on outdated, off-policy trajectories, as done in SAC, becomes infeasible. **To improve sample efficiency, instead of updating the policy and world model only once per learning iteration, as done in Lines 6 and 7 of Algorithm 1, we can update them for multiple epochs using the same batch of on-policy samples.** Following PPO [46, 47], we apply gradient masks to both the policy and world model to regulate parameter updates based on outdated

Algorithm 2 ROMBRL

```

1: Input: offline dataset  $-\mathcal{D}_\mu$ , # of training iterations  $-K$ , uncertainty range  $-\epsilon$ , learning rates  $-\eta_\theta, \eta_\phi, \eta_\lambda$ , # of training epochs  $-E_v, E_\theta, E_\phi, E_\lambda$ , update rate for the target network  $-\iota$ 
2: Obtain  $\bar{\phi} \in \arg \max_{\phi} \mathbb{E}_{(s,a,r,s') \sim \mathcal{D}_\mu} [\log P_\phi(s', r|s, a)]$ 
3: Initialize  $v, \bar{v}, \theta^1, \phi^1$ , and  $\lambda^1$  with  $\lambda^1 > 0$ 
4: Initialize the replay buffer:  $\mathcal{D} \leftarrow \emptyset$ , which is a queue with a limited capacity
5: for  $k = 1 \cdots K$  do
6:   Sample truncated rollouts  $\mathcal{D}_{\text{on}} \sim P(\cdot; \theta^k, \phi^k)$  with initial states randomly drawn from  $\mathcal{D}_\mu$ 
7:   Update  $\mathcal{D}$  with  $\mathcal{D}_{\text{on}}$ 
8:   Train  $Q_v$  and  $V_v$  for  $E_v$  epochs, according to Eq. (67), using samples from  $\mathcal{D}$ 
9:   Update the target network:  $\bar{v} \leftarrow \iota v + (1 - \iota)\bar{v}$ 
10:   $\theta' \leftarrow \theta^k, \phi' \leftarrow \phi^k, \lambda' \leftarrow \lambda^k$ 
11:  for  $e_\theta = 1 \cdots E_\theta$  do
12:    Sample rollouts from  $\mathcal{D}_{\text{on}}$  and state transitions from  $P_{\bar{\phi}} \circ \mathcal{D}_\mu(\cdot)$  for gradient estimation
13:     $\theta' \leftarrow \theta' + \eta_\theta \left[ \nabla_{\theta} \hat{J}(\theta', \phi^k) - \nabla_{\bar{\phi}}^2 \hat{\mathcal{L}}(\theta', \phi^k, \lambda^k)^T \hat{H}(\theta', \phi^k, \lambda^k) \nabla_{\phi} \hat{J}(\theta', \phi^k) \right]$ 
14:  end for
15:  for  $e_\phi = 1 \cdots E_\phi$  do
16:    Sample rollouts from  $\mathcal{D}_{\text{on}}$  and state transitions from  $P_{\bar{\phi}} \circ \mathcal{D}_\mu(\cdot)$  for gradient estimation
17:     $\phi' \leftarrow \phi' - \eta_\phi \nabla_{\phi} \hat{\mathcal{L}}(\theta^k, \phi', \lambda^k)$ 
18:  end for
19:  for  $e_\lambda = 1 \cdots E_\lambda$  do
20:    Sample state transitions from  $P_{\bar{\phi}} \circ \mathcal{D}_\mu(\cdot)$  for gradient estimation
21:     $\lambda' \leftarrow [\lambda' + \eta_\lambda \nabla_{\lambda} \hat{\mathcal{L}}(\theta^k, \phi^k, \lambda')]^+$ 
22:  end for
23:   $\theta^{k+1} \leftarrow \theta', \phi^{k+1} \leftarrow \phi', \lambda^{k+1} \leftarrow \lambda'$ 
24: end for

```

data. Specifically, the policy gradient mask for (s_t, a_t) within a trajectory τ is defined as:

$$m_t^\pi(\tau) = \begin{cases} 1, & \text{if } r_\theta(s_t, a_t) \hat{A}(s_t, a_t; \tau) \leq \text{clip}(r_\theta(s_t, a_t), 1 - \epsilon_c, 1 + \epsilon_c) \hat{A}(s_t, a_t; \tau) \\ 0, & \text{otherwise} \end{cases}$$

where $\epsilon_c > 0$ is the clipping rate, $r_\theta(s_t, a_t) = \frac{\pi_\theta(a_t|s_t)}{\pi_{\theta^k}(a_t|s_t)}$ is the importance sampling ratio, and $\hat{A}(s_t, a_t; \tau)$ is the generalized advantage estimation (GAE), computed based on a value function and the trajectory sample τ . The world model gradient mask $m_t^P(\tau)$ can be similarly defined by replacing $r_\theta(s_t, a_t)$ with $r_\phi(s_t, a_t, r_t, s_{t+1}) = \frac{P_\phi(r_t, s_{t+1}|s_t, a_t)}{P_{\phi^k}(r_t, s_{t+1}|s_t, a_t)}$ and substituting $\hat{A}(s_t, a_t; \tau)$ with $\hat{A}(s_t, a_t, r_t, s_{t+1}; \tau)$. In particular, given a trajectory $\tau = (s_0, a_0, r_0, s_1, \dots, s_l, a_l)$, the GAE at time step t can be computed as follows:

$$\begin{aligned} \hat{A}(s_t, a_t; \tau) &= \sum_{i=t}^{l-1} (\gamma \zeta)^{i-t} [r_i + \gamma V_v(s_{i+1}) - V_v(s_i)], \\ \hat{A}(s_t, a_t, r_t, s_{t+1}; \tau) &= \sum_{i=t}^{l-1} (\gamma \zeta)^{i-t} [r_i + \gamma Q_v(s_{i+1}, a_{i+1}) - Q_v(s_i, a_i)]. \end{aligned} \tag{66}$$

Here, $\zeta \in (0, 1]$ is a hyperparameter⁸; $\hat{A}(s_t, a_t, r_t, s_{t+1}; \tau)$ serves as an analogy to $\hat{A}(s_t, a_t; \tau)$, since for the world model $P_\phi(r_t, s_{t+1}|s_t, a_t)$, (s_t, a_t) is the "state" and (r_t, s_{t+1}) is the "action". **Notably, with the value functions, we can use truncated rollouts τ (with a horizon $l < h$) to compute policy/model gradients by replacing the return-to-go $\sum_{j=t}^{h-1} \gamma^j r_j$ with $\gamma^t \hat{A}(s_t, a_t; \tau)$ or $\gamma^t \hat{A}(s_t, a_t, r_t, s_{t+1}; \tau)$, effectively mitigating compounding errors that arise from long-horizon model predictions.** Unlike the policy, the value functions can be trained using off-policy samples

⁸When $\zeta = 1$, $\hat{A}(s_t, a_t; \tau) = -V_v(s_t) + r_t + \dots + \gamma^{l-1-t} r_{l-1} + \gamma^{l-t} V_v(s_l)$ and $\hat{A}(s_t, a_t, r_t, s_{t+1}; \tau) = -Q_v(s_t, a_t) + r_t + \dots + \gamma^{l-1-t} r_{l-1} + \gamma^{l-t} Q_v(s_l, a_l)$.

from a replay buffer. The objectives at iteration k are given by: ($V_{\bar{v}}$ is the target value network.)

$$\begin{aligned} \min_{V_v} \mathbb{E}_{s \sim \mathcal{D}} \left[(V_v(s) - \mathbb{E}_{a \sim \pi_{\theta^k}(\cdot|s)}[Q_v(s, a)])^2 \right], \\ \min_{Q_v} \mathbb{E}_{(s, a) \sim \mathcal{D}} \left[(Q_v(s, a) - \mathbb{E}_{(r, s') \sim P_{\phi^k}(\cdot|s, a)}[r + V_{\bar{v}}(s')])^2 \right]. \end{aligned} \quad (67)$$

As in PPO, we apply gradient masks to Eq. (9) to ensure that only selected state-action pairs contribute to the policy/model update, while the gradient information from all other pairs is masked out. Specifically, $\nabla_{\phi} J(\theta^k, \phi^k)$ in the 2nd line of Eq. (9) is substituted with:

$$\nabla_{\phi} J(\theta^k, \phi^k) = \mathbb{E}_{\tau \sim P(\cdot; \theta^k, \phi^k)} \left[\sum_{t=0}^{l-1} m_t^P(\tau) \gamma^t \hat{A}(r_t, s_{t+1}|s_t, a_t; \tau) \nabla_{\phi} \log P_{\phi'}(r_t, s_{t+1}|s_t, a_t) \right] \quad (68)$$

Also, $\nabla_{\theta} J(\theta^k, \phi^k)$ and $\nabla_{\phi\theta}^2 \mathcal{L}(\theta^k, \phi^k, \lambda^k)$ in the 1st line of Eq. (9) are substituted with:

$$\begin{aligned} \nabla_{\theta} J(\theta', \phi^k) &= \mathbb{E}_{\tau \sim P(\cdot; \theta^k, \phi^k)} \left[\sum_{t=0}^{l-1} m_t^{\pi}(\tau) \gamma^t \hat{A}(s_t, a_t; \tau) \nabla_{\theta} \log \pi_{\theta'}(a_t|s_t) \right], \\ \nabla_{\phi\theta}^2 \mathcal{L}(\theta', \phi^k, \lambda^k) &= \nabla_{\phi\theta}^2 J(\theta', \phi^k) = \mathbb{E}_{\tau \sim P(\cdot; \theta^k, \phi^k)} \left[\nabla_{\phi} \Psi(\tau, \phi^k) \left(\sum_{t=0}^{l-1} m_t^{\pi}(\tau) \nabla_{\theta} \log \pi_{\theta'}(a_t|s_t) \right)^T \right] \end{aligned} \quad (69)$$

To sum up, we propose using a multi-epoch update mechanism enabled by gradient masks to improve sample efficiency and adopting truncated rollouts based on value functions to mitigate compounding errors. We provide the detailed pseudo code as Algorithm 2. Definitions of the gradient updates in Lines 13, 17, 21 are available in Eqs. (9), (10), (11), (54), (64), (65), (68), and (69).

K Details of the Tokamak Control Tasks

Table 3: The state and action spaces of the tokamak control tasks.

STATE SPACE	
Scalar States	β_N , Internal Inductance, Line Averaged Density, Loop Voltage, Stored Energy
Profile States	Electron Density, Electron Temperature, Pressure, Safety Factor, Ion Temperature, Ion Rotation
ACTION SPACE	
Targets	Current Target, Density Target
Shape Variables	Elongation, Top Triangularity, Bottom Triangularity, Minor Radius, Radius and Vertical Locations of the Plasma Center
Direct Actuators	Power Injected, Torque Injected, Total Deuterium Gas Injection, Total ECH Power, Magnitude and Sign of the Toroidal Magnetic Field

Nuclear fusion is a promising energy source to meet the world’s growing demand. It involves fusing the nuclei of two light atoms, such as hydrogen, to form a heavier nucleus, typically helium, releasing energy in the process. The primary challenge of fusion is confining a plasma, i.e., an ionized gas of hydrogen isotopes, while heating it and increasing its pressure to initiate and sustain fusion reactions. The tokamak is one of the most promising confinement devices. It uses magnetic fields acting on hydrogen atoms that have been ionized (given a charge) so that the magnetic fields can exert a force on the moving particles [38].

The authors of [39] trained an ensemble of deep recurrent probabilistic neural networks as a surrogate dynamics model for the DIII-D tokamak, a device located in San Diego, California, and operated by General Atomics, using a large dataset of operational data from that device. A typical shot (i.e., episode) on DIII-D lasts around 6-8 seconds, consisting of a one-second ramp-up phase, a multi-second flat-top phase, and a one-second ramp-down phase. The DIII-D also features several real-time and post-shot diagnostics that measure the magnetic equilibrium and plasma parameters

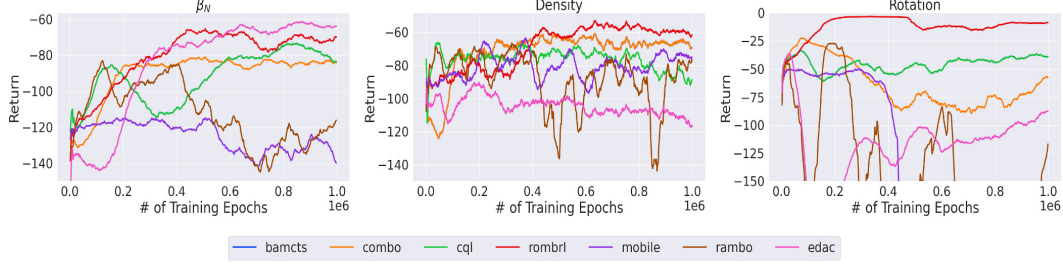


Figure 4: Evaluation results on Tokamak Control tasks. The figure shows the progression of episodic tracking errors over training epochs for the proposed algorithm and baseline methods. Solid lines indicate the average performance across multiple random seeds. For clarity of presentation, the curves have been smoothed using a sliding window, and confidence intervals are omitted.

with high temporal resolution. **The authors demonstrate that the learned model predicts these measurements for entire shots with remarkable accuracy. Thus, we use this model as a "ground truth" simulator for tokamak control tasks.** Specifically, we generate a dataset of 111305 transitions for offline RL by replaying actuator sequences from real DIII-D operations through the ensemble of dynamics models. Policy evaluation is conducted using a noisy version of this data-driven simulator to assess deployment robustness.

The state and action spaces for the tokamak control tasks are outlined in Table 3. For detailed physical explanations of them, please refer to [48, 49, 50]. The state space consists of five scalar values and six profiles which are discretized measurements of physical quantities along the minor radius of the toroid. After applying principal component analysis [51], the pressure profile is reduced to two dimensions, while the other profiles are reduced to four dimensions each. In total, the state space comprises 27 dimensions. The action space includes direct control actuators for neutral beam power, torque, gas, ECH power, current, and magnetic field, as well as target values for plasma density and plasma shape, which are managed through a lower-level control module. Altogether, the action space consists of 14 dimensions. **Following guidance from fusion experts, we select a subset of the state space: β_N and all profile states, as policy inputs, spanning 23 dimensions. The policy is trained to control five direct actuators: power, torque, total ECH power, the magnitude and sign of the toroidal magnetic field. For the remaining actuators listed in Table 3, we replay the corresponding sequences from recorded DIII-D operations.**

For evaluation, we select 9 high-performance reference shots from DIII-D, which span an average of 251 time steps, and use the trajectories of Ion Rotation, Electron Density, and β_N within these shots as targets for three tracking tasks. Specifically, β_N is the normalized ratio between plasma pressure and magnetic pressure, a key quantity serving as a rough economic indicator of efficiency. **Since the tracking targets vary over time, we also include the target quantity as part of the policy input.** The reward function for each task is defined as the negative squared tracking error of the corresponding quantity (i.e., rotation, density, or β_N) at each time step. Notably, for policy learning, the reward function is provided rather than learned from the offline dataset as in D4RL tasks; and the dataset (for offline RL) does not include the reference shots.